INVESTIGATION OF THE NATURE OF STRUCTURAL CHANGE IN 2014-T6 ALUMINUM ALLOY FROM MAGNETOMOTIVE VS. CONVENTIONAL METALWORKING

7-Month Progress Report

THE NATIONAL AERONAUTICS AND SPACE ADMINISTRATION
GEORGE C. MARSHALL SPACE FLIGHT CENTER
HUNTSVILLE, ALABAMA 35812

CONTRACT NO. NAS8-21254

SEPTEMBER 1, 1967 – APRIL 1, 1968

prepared by

Arthur D. Little, Inc.
15 ACORN PARK
CAMBRIDGE, MASSACHUSETTS 02140

Arthur D. Little, Inc.

ARTHUR D. LITTLE, INC.

15 Acorn Park

Cambridge, Massachusetts

Research & Development

Materials Section

7-Month Progress Report

September 1, 1967 - April 1, 1968

Prepared for George C. Marshall Space Flight Center

Huntsville, Alabama

CONTRACT NAS8-21254

INVESTIGATION OF THE NATURE OF STRUCTURAL CHANGE IN 2014-T6 ALUMINUM ALLOY FROM MAGNETOMOTIVE VS. CONVENTIONAL METALWORKING

ABSTRACT

The effect of deformation on the strengths of welded and sheet 2014-T6 aluminum has been measured. Deformation of the sheet aluminum was by magnetomotive and by explosive forming in an open die. Notched and unnotched tensile tests were performed at three temperatures, ambient, liquid nitrogen, and 350°F. Our tests showed no apparent differences in the strengths of the alloy deformed either magnetomotively or explosively, but a definite decrease in notch tensile strength for the worked sheet vs. the non-worked sheet. The welded plate or sheet was magnetomotively bulge formed, and also was hammered with the magnetomotive coil. Preliminary results of the strength tests on specimens cut from these plates and sheets are reported here and possible future work on welded plates is described.

TABLE OF CONTENTS

LIST OF TABLES

LIST OF FIGURES

A. INTRODUCTION

Magnetomotive working is an eloquent technique in which a pulsed current in a coil sets off a repulsive field in the workpiece. This process of forming has several distinct, interesting features that make it very attractive to a fabricating engineer for use in his shop. The equipment is portable, relatively simple to operate, requires little or no auxiliary tooling, can affect various amounts of metal movement without contact or visible damage to the workpiece. The process has demonstrated an ability to form shapes as well as to affect removal of distortion and to correct defective contours to acceptable dimensions.

A tantalizing problem exists, however, regarding process parameters that can be employed satisfactorily and simultaneously ensure reliable, acceptable performance of the magnetomotively worked structure. Material can be overworked or abused and caused to fail either immediately or subsequently by excessive application of force from any source. Therefore it is necessary to develop and provide adequate data to establish guidelines for appropriate application and to establish a process specification for magnetomotive working on Apollo structures. One of the first aims in the present work on 2014-T6 was to look for obvious trouble in overworked material and then to back off to a "reasonable" level for more extensive evaluation by appropriate tests. It should be noted here that results obtained on 2014-T6 would not be expected to apply to 2219- which inherently responds differently to cold work.

To give a complete picture of the effect of deformation, sheet has been deformed at high strain rates, with use of the magnetomotive coil, as well as with explosives and will be deformed at low strain rates, with hydrostatic pressure. The high strain studies will be reported on here, but the low strain rate studies will have to wait for a later report; since the hydrostatic pressure forming will be done within the next few months.

B. STRENGTHS OF BULGED UNWELDED DOMES

Aluminum alloy plates, 2014-T6, were bulge-formed in an open die of 11" diameter at NASA Marshall Space Flight Center with their magnetomotive coil, as well as explosively, and were sent to us for evaluation. Our tests included microscopy hardness, tensile, and notch tensile of specimens prepared from the formed sheets. In order to simulate service conditions, specimens were tested at ambient temperature, in liquid nitrogen, and at 350°F. In addition to the strength tests, thin-out and profile of the sheets were measured. The following section contains the results of our evaluation.

TESTING METHODS

The length of the tensile specimen was chosen to fit inside the bulged area of the dome. For convenience of testing, the tensile specimen was held with a pin insert. This was the only way that we could grip the curved tensile specimens from the bulged sheets with a minimum introduction of bending moments at the ends. The specimen shape was arrived at by trial and error until we had a shape that caused fracture to occur in the center of the gauge section. The specimen was also designed with large ends so that no apparent opening of the pin hole occurred during testing. The final specimen size used throughout our tests is drawn in Figure 1. This specimen shape was used on all the sheets sent to us. The notch tensile specimen was identical to the tensile specimen except that a notch was introduced on both sides of the mid-section, see Figure 2. This notch has an included angle of 60°, is 0.075 in depth, a root radius less than or equal to 0.001 in., with a stress concentration factor $K \cong 10$ $K = 1 + \left(\frac{c}{a}\right)^{1/2}$, and c is the notch depth, a is the radius of curvature at the tip of the notch.

All the tensile specimens were positioned on the bulged unwelded sheet like that shown in Figure 3. Specimens are placed so that the top end of the gauge section is 2 1/4" from the peak of the bulged sheet. From one dome four specimens can be cut, two parallel to, and two perpendicular to the rolling direction of the sheet. This direction of the tensile specimen was recorded for all the specimens.

The test apparatus used for the cryogenic temperature was simply constructed but reliable. The specimen is suspended underneath the crosshead and is directly immersed in liquid nitrogen. The top of the specimen is connected by a rod and universal joint to the load cell. After immersing the specimen in the bath, it sat until appreciable bubbling stopped, then it was pulled.

The elevated temperature tests were done in air, with the specimen in a Missimers FT 18 Furnace. Again, the specimen was attached to the crosshead with a universal joint. The alloy was allowed to sit for one hour before it was pulled.

Besides the strength determinations, macro hardness measurements were made of the aluminum sheets. Specimens were cut from the sheet and the cross-section was given a metallographic polish before the hardness indentations were made. Due to the small cross section of the sheet, only one indentation could be made throughout the width of the section, and this tended to limit the number of indentations. However, the number of indentations made were sufficient to show the trends. Profile measurements were made on the formed sheets with a travelling micrometer, and thin-out was measured on sections cut from the sheets.

RESULTS OF TESTS ON FORMED ALUMINUM SHEETS

The differences in profile between the magnetomotively and explosively formed aluminum sheets of 1/8" thickness are shown in Figures 4 through 7. While Figures 8 through 11 give the thicknesses of these sheets. It is seen that the magnetomotively formed sheets have a secondary dome at the center while those explosively formed do not. We took the tensile specimens out of an area of the magnetomotively formed sheets which did not contain the secondary dome. Thin-out was greater for the sheets magnetomotively formed than for those explosively formed. The reason for this is probably due to the formation of the secondary dome on the sheets.

Complete results on the tensile and notch tensile determinations are given in Figures 12 through 16. Data used for these curves is given in Tables I through IX. The yield strength was measured at 0.2% offset strain, and the elongation was measured on the fractured specimen over a 1" gauge length. It should be noted that if the elongation were also determined from the Instron chart, the value agreed with that measured on the specimen. This shows that the plastic elongation of the specimen takes place only within the gauge section of the tensile specimen.

When relating the data from the flat specimens with that from the curved ones, the trends in the data should be noted. This is more important than a comparison of the absolute values. The reason is that the curved specimens from the bulged sheets are not free of bending moments while pulled in tension. These moments act on the specimen to straighten it during pulling. This bending moment causes yielding to occur at a lower apparent stress for the curved specimens than for the flat specimens.

Hardness measurements on these deformed sheets showed that there is no apparent change in hardness due to forming. The hardness of the deformed and undeformed regions of the alloy are 82 RB. Likewise, ultimate strength of this -T6 temper was little affected by forming, however notch strength was definitely decreased by forming.

It should be noted that there is no difference in the microstructure of the sheet in both the deformed or undeformed areas. This observation was made with both transmission electron microscopy and optical microscopy on specimens cut from sheet II.* This sheet was deformed magnetomotively to a depth of 1.72 in., about 1/2 in. deeper than the bulged sheets from which the tensile specimens were cut. This deformation represents the greatest amount which a sheet received.

No tensile specimens were taken from this sheet, since the curvature of the specimen is so large, and a large bending moment would be introduced during pulling.

*See Appendix A for a description of the method used, and electron micrographs of the deformed and undeformed areas.

EFFECT OF PRE-STRAIN ON NOTCH STRENGTH OF FLAT SHEET

The effect of high strain-rate deformation on notch strength was determined in this program; however, it was also of interest to know the effect of slow strain-rate deformation on notch strength. We performed tests in which the flat tensile specimen was pulled to a certain plastic strain, unloaded, then notched, and repulled. The area of the specimen used in the calculation of notch strength was corrected for the slight change in shape due to the initial tensile loading. The results of this study are shown in Figure 17 and the tabulated values are given in Table X. Apparently, the initial pre-strain lowers the notch strength, but the notch strength seems to drop at a decreasing rate as the pre-strain is increased. Although these determinations were exploratory, the results were interesting and possibly should be extended to measurements at other temperatures.

C. STRENGTHS OF THE WELDED PLATES AND SHEETS

In the final part of this program we investigated the properties of welded plates and sheets. These panels were prepared by NASA and sent to us for our studies. Two different approaches were used by NASA to deform the plates or sheets. In one, a 0.125 in. thick 2014-T6 aluminum sheet was welded along the mid-length from two half sections, then bulge formed magnetomotively similarly to the unwelded sheets. This sheet, 5W, was deformed but not enough to cause visible cracking, as determined by radiographic observation. A similar type of sheet, 6W, was also sent for observation but its level of deformation was sufficient to cause cracking along the length of the weld. In the other approach, a thicker welded plate (plate C) 0.270 in. thick, was prepared at NASA; however, this panel was magnetomotively worked to correct contour faults such as mismatch and peaking associated with welding. That is, the plate was magnetomotively hammered at various locations to correct the contour. Two settings of the energy bank for the coil were used, 3.5 and 4.0 K.V., to determine the effect of the level of deformation on weld strength.

Tests performed on the weld were tensile, notch tensile, and hardness. The tensile specimen was similar to that given in Figure 1 with the notch location in the center of the weld metal. This location had been established by previously noting that the fractured unnotched tensile specimens from the welds with the bead removed flushed broke in the weld metal. Since this zone is the weakest area of the weld, it was chosen for the notch location. Hardness measurements were made on the cross section of the plate on a section transverse to the long length of the weld. Thus, weld metal, the heat-affected zones, and unaltered metal were contained on this cross section. Figure 18 is a schematic layout of the fracture and tensile specimens on sheet 5W. This choice of specimen locations allowed us to test both deformed and undeformed areas.

The weld metal above the surface of the sheet and plate was removed by filing and sanding so that the metal was flush with the surface. This made the determinations of strengths easier; since the cross section of the plate or sheet was known.

RESULTS OF THE TESTS ON THE WELDED PLATES AND SHEETS

The strength tests on the welds are given in Tables XI and XII, and the hardness determinations in Tables XIII through XV. In addition, Figures 19 through 21 show the location of the hardness indentations. It is difficult to draw generalities from the strength tests; since there is little data. There seems to be no apparent effect of the deformation of the welds on the strength levels. Of course, more data would be needed to confirm this point. An interesting result occurred from the test of Specimen 5 in Table XI. This specimen was cut from an area which showed line of porosity on the radiograph. The effect of this porosity on tensile properties was to lower the total elongation with no effect on the yield or tensile strength. In these tables, specimens are given for which there is no associated data. Unfortunately these are specimens which were prepared to be tested, but suffered errors in handling on the Instron.

The main value of the hardness measurements is to show the extent of the heat-affected zone. For the 1/8 in. sheet, the heat-affected zone extends out 1/4 to 1/2 in. from the edge of the weld metal (the fusion zone). For the thicker 0.270 in. plate the heat-affected zone extends 1/2 to 3/4 in. from the edge of the weld metal. This distance is that in which the hardness reaches that of the unaffected metal, i.e., RB 81. There was no apparent effect of deformation of sheet 5W on its hardness, in the region of the -T6 temper, but there may be any increase of hardness in the partially annealed zone.

The tensile fractures of the welds were observed to go through the weld metal, not through the fusion zone. This observation was made on etched fracture surfaces from specimens of plates 5W and C. This does not mean that the fracture could not go through the fusion zone, or possibly begin there, in some cases. An example of a fracture going through the weld metal is shown in Figure 22 for specimen 2 of sheet 5W. As mentioned previously, this observation of the crack path was used to place the notch in the weld zone of the notched tensile specimen.

The fracture in sheet 6W, which broke on forming, also appeared to run through the weld metal, this observation was made from a cross section through the weld metal and transverse to the length of the weld. Of course, there is so much wandering of the fracture along the length of the weld that it is difficult to generalize about the location of the fracture.

D. DISCUSSION

There were two types of measurements made in this program. In one, the effect of deformation, produced by magnetomotive or explosive forming, on the strength of unwelded 2014-T6 aluminum sheet was measured. In the other, preliminary measurements were made on the effect of magnetomotive forming or hammering on the strengths of 2014-T6 welds. The measurements of the sheet and welded aluminum are quite distinct and will be treated separately in this discussion.

STRENGTHS OF FORMED UNWELDED 2014-T6 SHEET ALUMINUM

The measurements made on the sheets compared the strengths of this alloy formed both explosively and magnetomotively. The general result from our work is that both forming methods caused the aluminum alloy to have comparable strengths at the same level of bulging. There is no apparent effect of the type of high strain-rate deformation on strength. Although we have not tested the 2014-T6 alloy after slow strain rate loading, we expect that the strength is unaffected by the rate of loading. The reason for this based on results previously found by Holt et al (1). They found that 6061-T6 and 7075-T6 aluminum alloys showed no strain-rate dependence of the flow stress, up to strain rates, of 10^3 in/in/sec. Apparently, the flow stress of the T6 alloy is insensitive to strain rate. This result, though did not hold for the 0 temper.

To test the concept that strain rate does not affect the flow stress of 2014-T6 plates will be hydrostatically-pressure formed by NASA. These plates will be tested by us, but the results will have to be written as a separate report.

An inherent difficulty with the present study, was the use of the curved tensile specimen cut from the bulged plate or sheet. The bending moments caused during pulling made it impossible to relate flow stresses of the bent specimens with those of the flat control specimens. Even though this could not be done, at least we were able to relate the flow stresses of specimens cut from sheets and bulged to the same level.

STRENGTHS OF THE WELDED PLATES

The results of these tests are complete enough to comment on the level of weld strength, but too incomplete to comment on the effect of deformation on weld strength. On the latter point, the work needed will be discussed at the end of this report. On the former, our recorded strengths for both the bulged welded dome and the welded plate are less than those recorded by MSFC (2). Their results are yield strengths 34-36 ksi, tensile strengths 52-54 psi, and elongations 7-8% over 1 inch gauge length. These results are summary data from both tensile tests on magnetomotively deformed and also undeformed welds. There was no apparent difference in the strength of the deformed and undeformed welds. These values should be compared to the lower strengths of the welds reported by us: yield strengths 29-34 ksi, tensile strengths 42-49 ksi, and elongations 4.5 - 5.5% over 1 inch gauge length.

To obtain better agreement with the data compiled at NASA, we will also use a similar gauge length to that used, i.e., 2 inches. The fact that we used a flush bead instead of a shaved bead may have caused the strengths recorded by us to be lower than those determined by NASA.

E. FUTURE WORK

The study of the fracture strengths of welds needs more effort, since our present results are incomplete. A suggested program has already been submitted in detail to Marshall Space Flight Center. This program consists of an investigation of the strengths of welded plates in which controlled weld distortions have been made. These distortions would be peaking, mismatch, or possibly combinations of these distortions. The maximum magnitude of the distortions would be about that experienced in welding of the Saturn V tank. The distortions would be removed by magnetomotive hammering. Both tensile and notch tensile tests will be made on the welded plates at ambient and liquid nitrogen temperatures. Since both 2014 and 2219 are used in the vehicle, both alloys will be tested in this program. By the end of this program we should have a complete understanding of the effect of magnetomotive hammering on the behavior of welds. The notch strength data should be fairly indicative of the subsequent integrity of similarly worked hardware.

F. CONCLUSIONS

The fracture strengths and notch tensile strengths of specimens taken from bulged sheets of 2014-T6 formed magnetomotively and explosively are similar. Measurements were made at ambient temperature, -320°F (liquid nitrogen) and 350°F. There was considerable scatter in the data, and more work is needed to differentiate the tensile and notch tensile strengths of specimens which were pulled in directions parallel and perpendicular to the rolling direction of the sheet.

The notch strength of the alloy depends upon the prestrain. With increasing prestrain the notch strength drops, but there was indication that the notch strength drops at a decreasing rate. The scatter in the data was significant and more work needs to be done to check the latter point.

Although we were unable to measure the strain of the sheets with the photoresist grid, since the lines of the grid were too wide, we believe that this technique should be used. This is an eloquent way to measure the strain imposed by the deformation. It should be a fairly simple task to develop this technique so that it is useable.

The information from the tensile and notch tensile tests of the welds have been very informative. The preliminary information from these tests show that these tests are an ideal way to study the effect of magnetomotive working on the welds.

G. APPENDIX

The following appendices include work which was performed during the contract, but which were separate from the main part of this program which dealt with strength tests. They are included here for record of the work performed.

APPENDIX A - TRANSMISSION ELECTRON MICROSCOPY

Transmission electron microscopy was used to supplement the optical microscopy studies of the deformed and undeformed regions of the bulged plates. We tried electron microscopy, since optical microscopy did not reveal any apparent influence of deformation on structure for both magnetomotively and explosively worked samples. Since there is so much fine structure in the T6 condition of the 2014 alloy, due to the precipitates, it was felt that transmission electron microscopy would be an ideal way to study this alloy.

The specimen thinning for electron microscopy was straightforward, there is no difficulty in preparing the 2014-T6 alloy for electron microscopy. Preparation was begun by cutting 1/8" thick sections out of the cross section of sheet 11. The sides of the cut section were parallel to the cross section of the sheet, and also parallel to the diameter of the sheet. The cut section was reduced in cross section to about 0.020" by hand lapping, then both sides of the specimen were metallographically polished to ensure that the sides were flat. We found that the success in thinning the specimen depends upon having the sides flat, otherwise the thinning would proceed too rapidly in some areas of the specimen and the thin film would not be transparent. After this metallographic preparation the specimen was thinned electrolytically in a solution of four parts methanol and one part perchloric. This solution is prepared by cooling the methanol to -10°C before adding the percholoric. The specimen is also thinned at this temperature. The voltage-current settings used for thinning were on the plateau customarily used.

Specimens were taken out of the peak, or worked region of plate II, which had been deformed magnetomotively, as well as the undeformed area of the same plate outside the circumference of the die.

Transmission electron micrographs of the thin sections of the sheet are shown in Figure 23A, undeformed region, and 23B, deformed region of plate II. As far as we could tell from these micrographs and overall examination of these thin films in the electron microscope, there is no apparent structural difference between the worked and unworked areas of this sheet. It is difficult to find any changes, since the precipitate dominates the structure.

For a detailed examination of the effect of the high strain rate working on structure, it would be better to use a solution treated sheet. For this condition there would be no precipitate structure, and it should be easier to see defects generated by the loading.

APPENDIX B - MICROSTRAIN STUDIES

As requested, microstrain determinations were attempted on our standard tensile specimens, although we had little success with the technique used. We used an Instron extensometer which was mounted directly on the specimen. Unfortunately, the noise level with this extensometer, used with a Keithley microvoltmeter for amplification was too high for us to detect strains of less than 5×10^{-5}. Thus the extensometer was too insensitive for microstrain work.

Instead of using an extensometer, we should have used a bonded strain gauge. We became aware of work supported by Goddard Space Flight Center, in which offset yields at 10^{-6} strain were determined for non-ferrous alloys, with the use of bonded strain gauges. The report describing this study (3) gives a good description of the technique used. If more microstrain determinations are to be made, the method should be similar to that described in this paper.

APPENDIX C - GRID MARKINGS ON SHEETS FOR DETERMINATION OF STRAIN

In order to determine the strain during magnetomotive forming, a set of photo-resist grids was put on several 2014-T6 alloy sheets. From the spacing of the grids, we had hoped to determine the permanent strain of deformation. We found that the lines of the grid were too coarse and we were not able to measure the permanent set. It certainly would not be difficult to use the grid to measure the permanent set if the grid lines had been finer. Instead of etching the grid on the sheets to find out if a permanent set can be measured, it would be simpler to put a grid on a tensile specimen which can be pulled. There can be experimentation with the grid so that the proper grid can be made. After the best grid has been developed, it can be used on the sheets.

TABLE I

STRENGTHS OF 2014-T6 1/8" SHEET TESTED AT ROOM TEMPERATURE

Unnotched U Notched N	Parallel P Transverse T to R.D.	Smooth Tensile Yield Strength ksi 0.2% offset	 Ultimate Strength ksi	 Elongation % in 1"	Notch Strength ksi $k_t = 10$
U	P	61.6	67.0	13.6	
		63.5	71.8	14.2	
		62.0	70.5	14.1	
U	T	60.6	72.5	13.5	
		60.8	73.0	13.1	
N	P				73.0
					70.8
					67.5
					69.3
					70.0
N	T				66.1
					66.4

TABLE II

STRENGTHS OF FLAT SPECIMENS TESTED AT LIQUID NITROGEN TEMPERATURE

Unnotched U Notched N	Parallel P Transverse T to R.D.	Yield Strength ksi 0.2% offset	Ultimate Strength ksi	Elongation % in 1"	Notch Strength ksi $k_t \cong 10$
U	P	86.0	87.5	14.35	
U	T	72.3	86.5	14.5	
		71.5	86.6	13.9	
N	P				73.2
N	T				79.0
					69.8

TABLE III

STRENGTHS OF FLAT SPECIMENS TESTED AT 350°F

Unnotched U Notched N	Parallel P Transverse T to R.D.	Yield Strength ksi 0.2% offset	Ultimate Strength ksi	Elongation % in 1"	Notch Strength ksi $k_t \cong 10$
U	P	48.6	51.5	13.6	
U	T	47.5	50.5	12.4	
N	P				59.0
N	T				57.0

TABLE IV

STRENGTHS OF MAGNETOMOTIVELY FORMED 2014-T6 1/8" SPECIMENS TESTED AT ROOM TEMPERATURE

Plate Number	Unnotched U Notched N	Parallel P Transverse T to R.D.	Yield Strength ksi 0.2% offset	Smooth Tensile Ultimate Strength ksi	Elongation % in 1"	Notch Strength ksi $k_t \cong 10$
12	U	P	60.2	70.4	13	
21			58.0	72.5	13.3	
23			57.3	72.5	13.0	
21	U	T	59.3	73.3	11.2	
23			59.5	73.5	11.9	
21	N	P				57.4
23						51.4
23	N	T				54.0

TABLE V

STRENGTHS OF MAGNETOMOTIVELY FORMED SPECIMENS TESTED AT LIQUID NITROGEN TEMPERATURE

Plate Number	Unnotched U Notched N	Parallel P Transverse T to R.D.	Yield Strength ksi 0.2% offset	Ultimate Strength ksi	Elongation % in 1"	Notch Strength ksi $k_t \geq 10$
25	U	P	66.0	87.4	11.7	
22			72.0	88.3	13.0	
25	U	T	65.0	86.6	13.6	
22			71.4	88.3	11.3	
25	N	P				61.8
22						53.5
25	N	T				50.8
22						52.7

TABLE VI

STRENGTHS OF MAGNETOMOTIVELY FORMED SPECIMENS TESTED AT 350°F

Plate Number	Unnotched U Notched N	Parallel P Transverse T to R.D.	Yield Strength ksi 0.2% offset	Ultimate Strength ksi	Elongation % in 1"	Notch Strength ksi $k_t \geq 10$
14	U	P	42.2	48.5	14.15	
27			43.0	48.7	10.8	
14	U	T	39.5	47.6	12.5	
27			39.6	47.8	8.7	
14	N	P				50.0
27						51.5
14	N	T				49.1
27						50.5

TABLE VII

STRENGTHS OF EXPLOSIVELY FORMED 2014-T6 1/8" SPECIMENS TESTED AT ROOM TEMPERATURE

Plate Number	Unnotched U Notched N	Parallel P Transverse T to R.D.	Yield Strength ksi 0.2% offset	Ultimate Strength ksi	Elongation % in 1"	Notch Strength ksi $k_t \cong 10$
16	U	P	55.5	71.8	14.1	
19			53.5	71.7	14.1	
16	U	T	54.2	72.7	11.9	
14			55.5	72.5	12.3	
19	N	P				51.3
14						50.3
19	N	T				51.5
14						48.0

TABLE VIII

STRENGTHS OF EXPLOSIVELY FORMED SPECIMENS TESTED AT LIQUID NITROGEN TEMPFRATURE

Plate Number	Unnotched U Notched N	Parallel P Transverse T to R.D.	Yield Strength ksi 0.2% offset	Ultimate Strength ksi	Elongation % in 1"	Notch Strength ksi $k_t \geq 10$
10	U	P	67.5	86.1	14.9	
9			85.0	88.2	11.7	
10	U	T	65.6	86.6	12.5	
9			61.7	86.0	13.7	
10	N	P				55.4
9						57.5
10	N	T				57.6
9						53.0

TABLE IX

STRENGTHS OF EXPLOSIVELY FORMED SPECIMENS TESTED AT 350°F

Plate Number	Unnotched U Notched N	Parallel P Transverse T to R.D.	Yield Strength ksi 0.2% offset	Ultimate Strength ksi	Elongation % in 1"	Notch Strength ksi $k_t \leq 10$
15	U	P	39.5	49.6	13.5	
29			41.6	49.6	13.0	
15	U	T	39.5	50.6	13.8	
29			39.5	50.3	13.4	
15	N	P				57.4
29						54.9
15	N	T				47.5
29						48.5

TABLE X

NOTCH STRENGTH OF PRE-STRAINED 2014-T6 1/8" TENSILE SPECIMENS TESTED AT ROOM TEMPERATURE

No.	ε in %	σ y s	σ Notch
	0		70,200
6ε	0.39	66,100	70,200
13ε	0.85	67,100	67,800
11ε	0.98	67,200	69,200
14ε	1.08	67,100	67,200
15ε	1.08	67,100	68,200
12ε	1.18	67,000	67,000
9ε	1.95	68,200	65,700
7ε	1.99	68,200	63,500
10ε	2.20	68,100	62,700
8ε	2.25	68,200	64,700
1ε	4.6	74,500	63,000
2ε	4.6	74,200	57,700
3ε	4.7	74,200	63,000
4ε	4.9	74,700	57,800
5ε	5.1	74,500	64,300

TABLE XI

STRENGTHS OF WELD SPECIMENS FROM MAGNETOMOTIVE DEFORMED WELDED 2014-T6 1/8"
PLATE C

Specimen	Undeformed U Deformed D	Unnotched U Notched N	Yield Strength psi 0.2% offset	Tensile Strenght or Notch Strength(*) psi	Elongation in 1" %
1A	U	U	31,800	49,500	5.44
2A	U	N			
3A	U	N		40,400	
1	D-3.5 K.V.	U	29,000	42,500	4.34
3	D-3.5 K.V.	U	34,200	49,200	4.44
2	D-3.5 K.V.	N		42,000	
4	D-3.5 K.V.	N		42,400	
5*	D-4 K.V.	U	34,200	45,900	2.68
6	D-4 K.V.	N		43,300	
7	D-4 K.V.	N		43,600	

----

*Specimen contained lined up porosity at weld interface shown on radiograph

(*)Notch is located at center of weld metal

TABLE XII

STRENGTH OF WELD SPECIMENS FROM THE MAGNETOMOTIVELY BULGED WELDED 2014-T6 1/8" SHEET 5W

Specimen	Undeformed U Deformed D	Unnotched U Notched N	Yield Strengh psi 0.2% offset	Tensile Strength or Notch Strength psi $k_t \geq 10$	Elongation in 1" %
1	U	U	35,000	49,200	6.3
6	U	N		39,500	
2	D	U	30,600	42,000	3.44
3	D	U	33,300	41,000	4.15
4	D	N			
5	D	N		38,300	

Specimens read 1 through 6 from one edge of plate to the other. That is, the pairs 3-4, 2-5, and 1-6 are symmetrically placed about the peak.

TABLE XIII

HARDNESS OF WELDED PANEL 5W IN UNDEFORMED REGION SPECIMEN I

Location Weld Metal or Distance From Fusion Zone	Hardness R_B
Weld Metal	34
0 (Fusion Zone)	58
0.027 in.	66
0.082 in.	58
0.258 in.	64
0.396 in.	79
0.515 in.	81

TABLE XIV

HARDNESS OF WELDED PANEL 5W IN DEFORMED REGION, SPECIMEN 3

Location Weld Metal or Distance From Fusion Zone	Hardness R_B
Weld Metal	42
0 (Fusion Zone)	61
0.03 in.	68
0.103 in.	63
0.230 in.	63
0.360 in.	81
0.473 in.	82
0.610 in.	82

TABLE XV

HARDNESS OF WELDED PLATE C AS WELDED

Location Weld Metal or Distance From Fusion Zone	Hardness R_B
Weld	57
0 (Fusion Zone)	65
0.046	72
0.140	61, 67
0.196	59
0.304	63
0.462	73
0.615	78
0.750	80
0.895	81

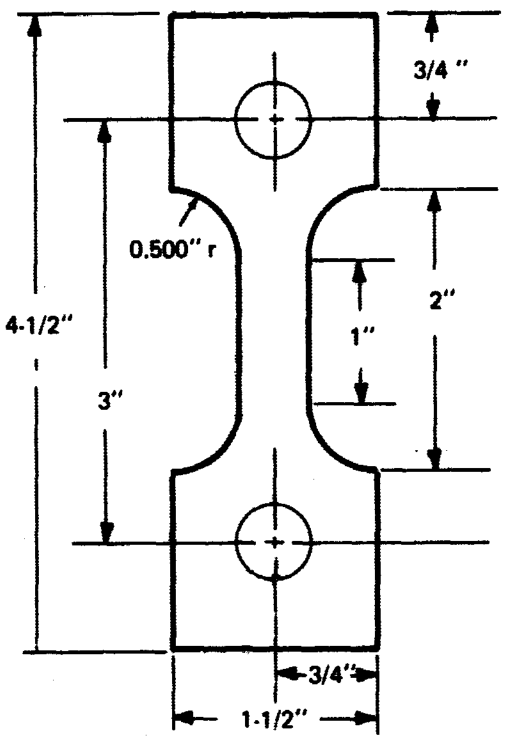

Hole Size 0.500 ± .0005"

Gauge Section Width 0.500 ± .0005"

FIGURE 1 ENGINEERING DRAWING OF TENSILE SPECIMEN IN GAUGE SECTION, THE SIDES ARE PARALLEL

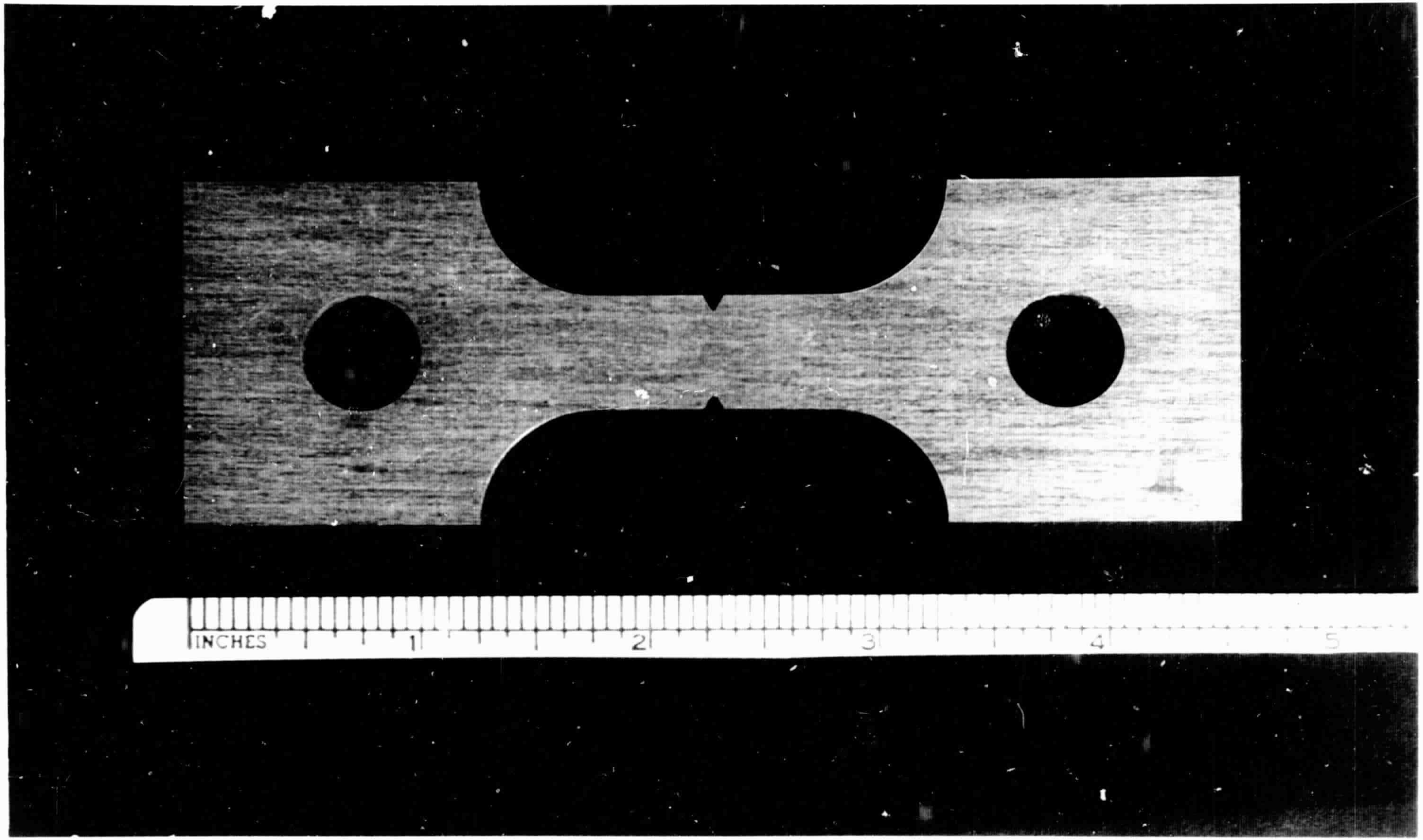

FIGURE 2 PHOTOGRAPH OF NOTCHED TENSILE SPECIMEN

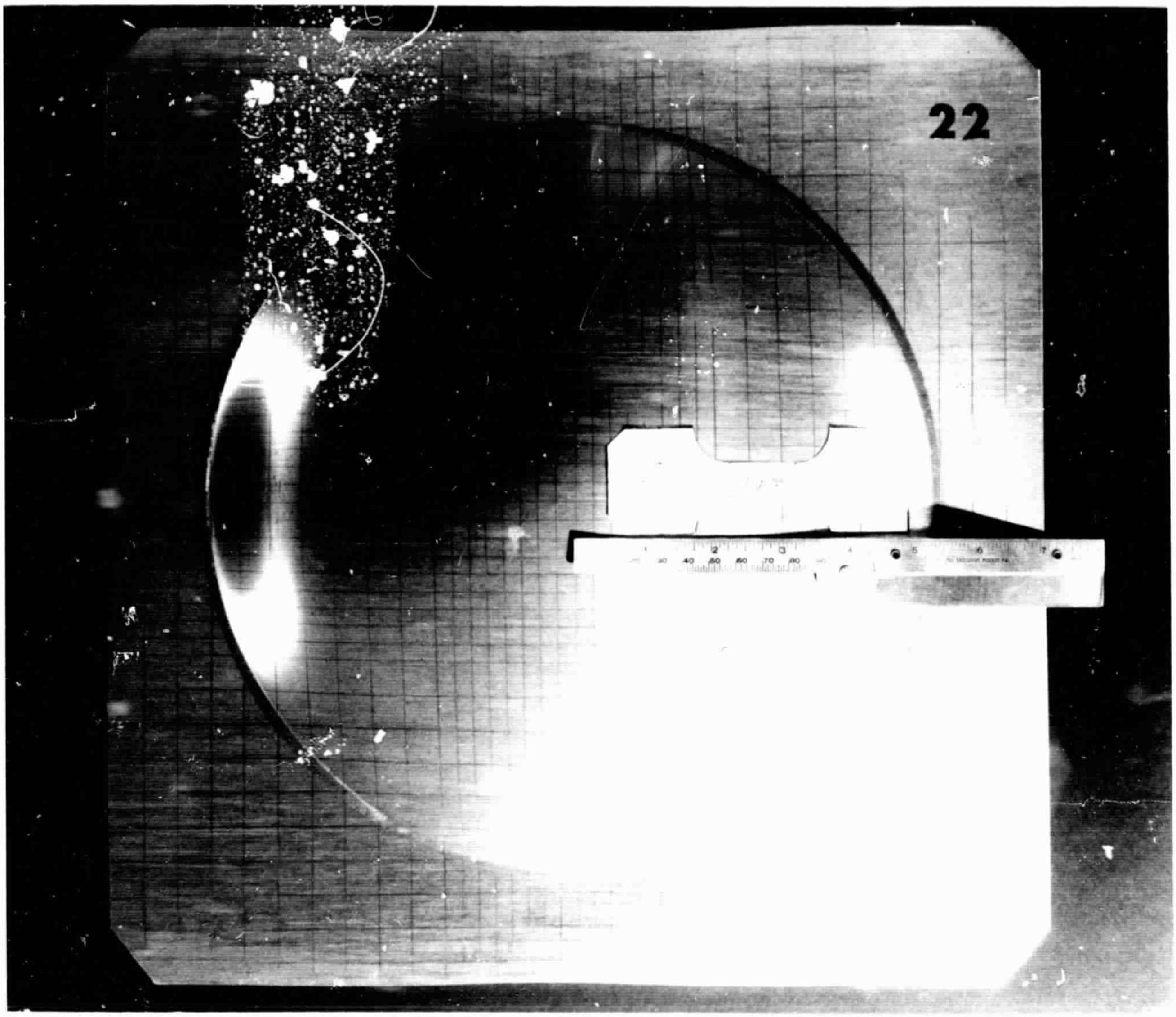

FIGURE 3 POSITION OF TENSILE SPECIMEN ON BULGED DOME

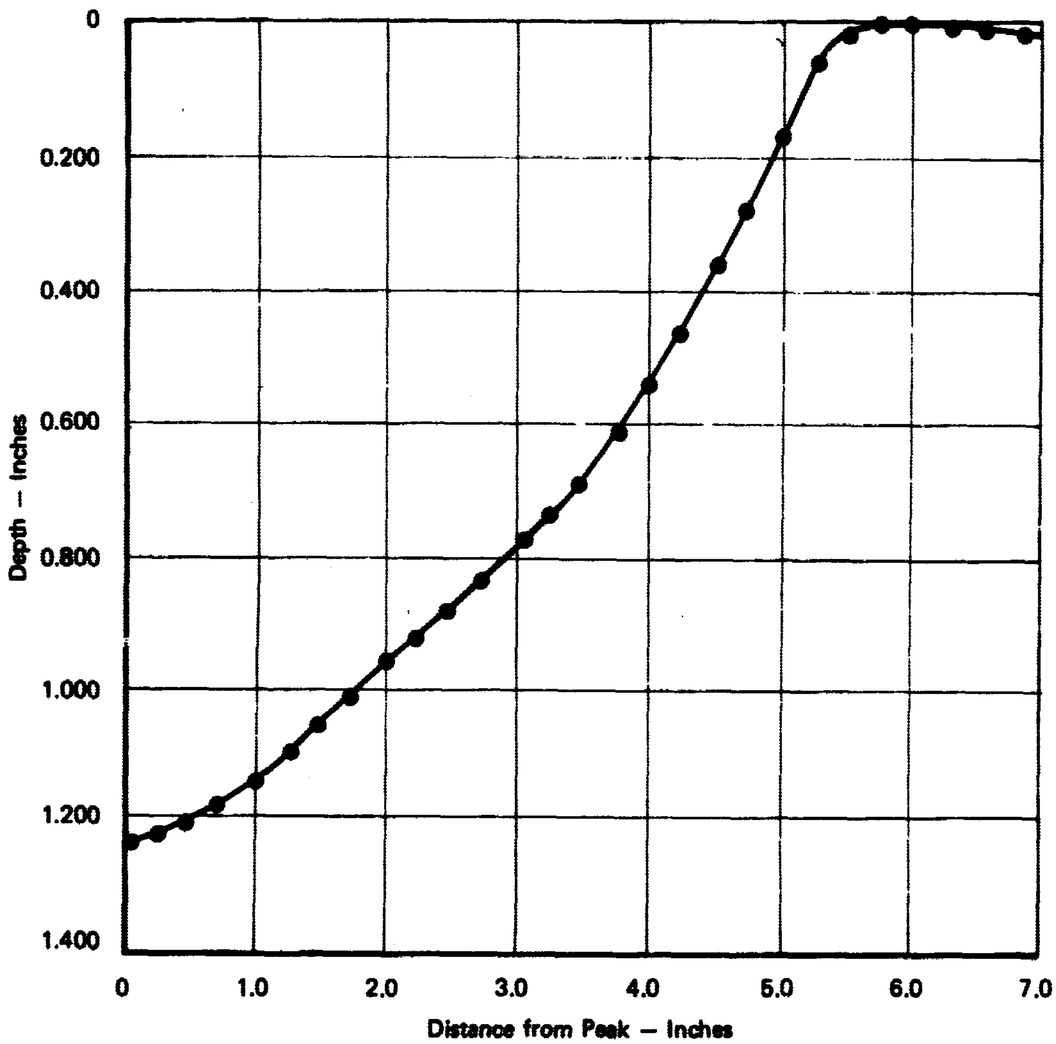

FIGURE 4 PROFILE OF MAGNETOMOTIVELY FORMED SHEET NO. 14 TAKEN PARALLEL TO ROLLING DIRECTION ON THE CONCAVE SURFACE

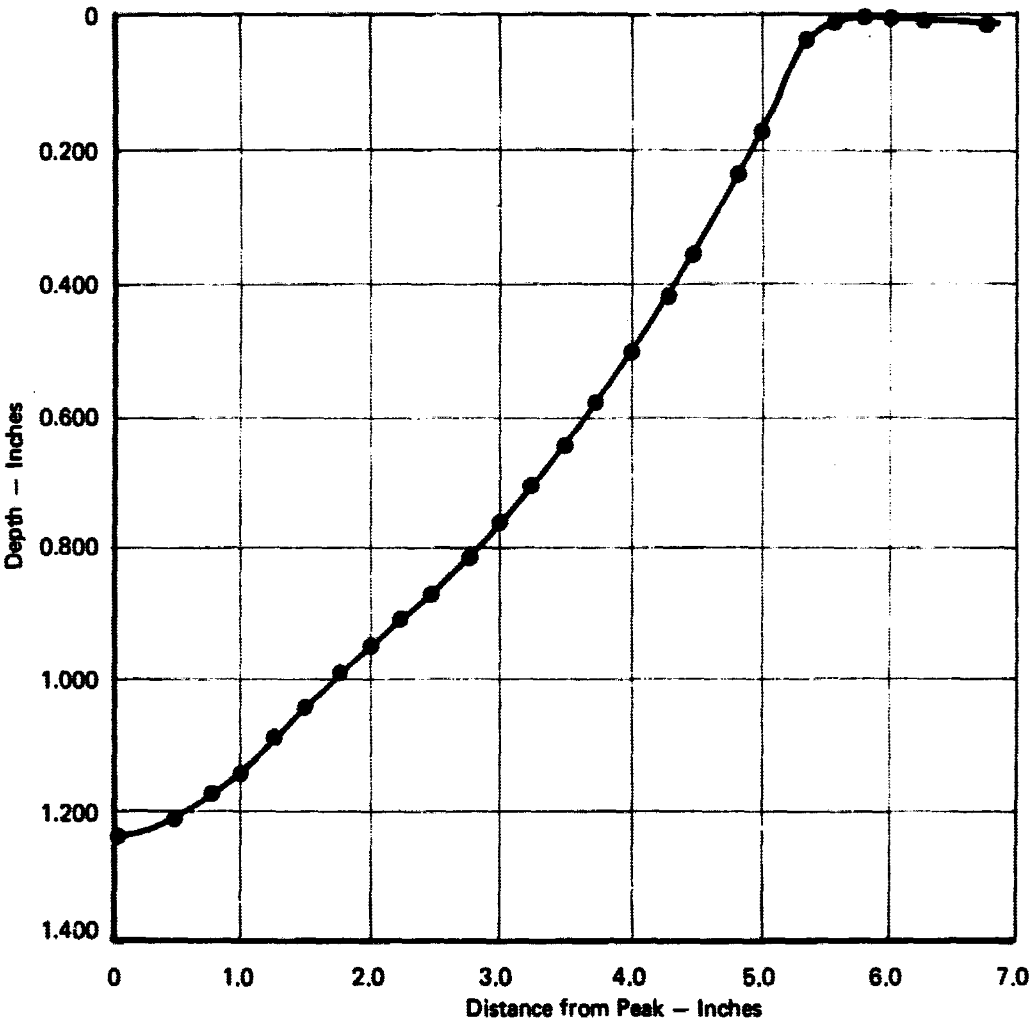

FIGURE 5 PROFILE OF MAGNETOMOTIVELY FORMED SHEET NO. 14 TAKEN TRANSVERSE TO ROLLING DIRECTION ON THE CONCAVE SURFACE

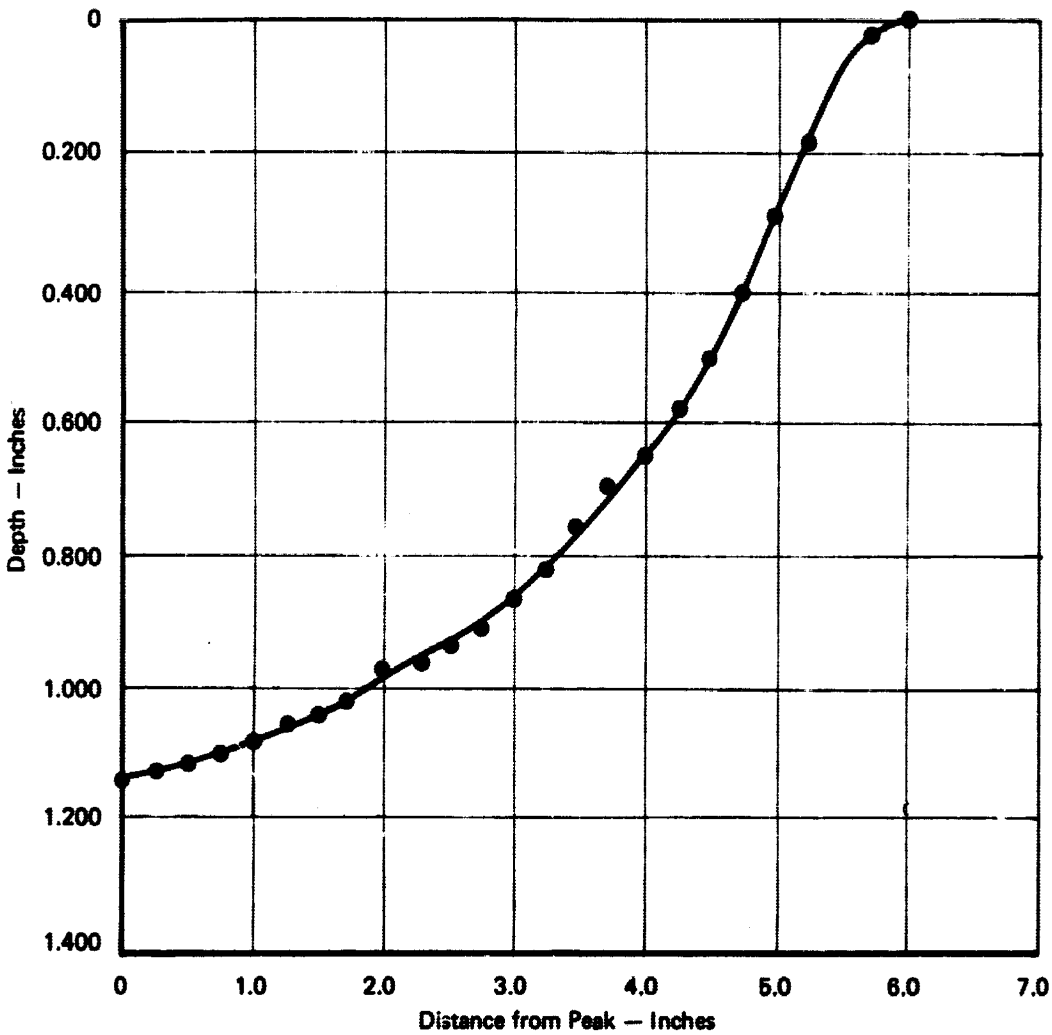

FIGURE 6 PROFILE OF EXPLOSIVELY FORMED SHEET TAKEN PARALLEL TO ROLLING DIRECTION ON THE CONCAVE SURFACE

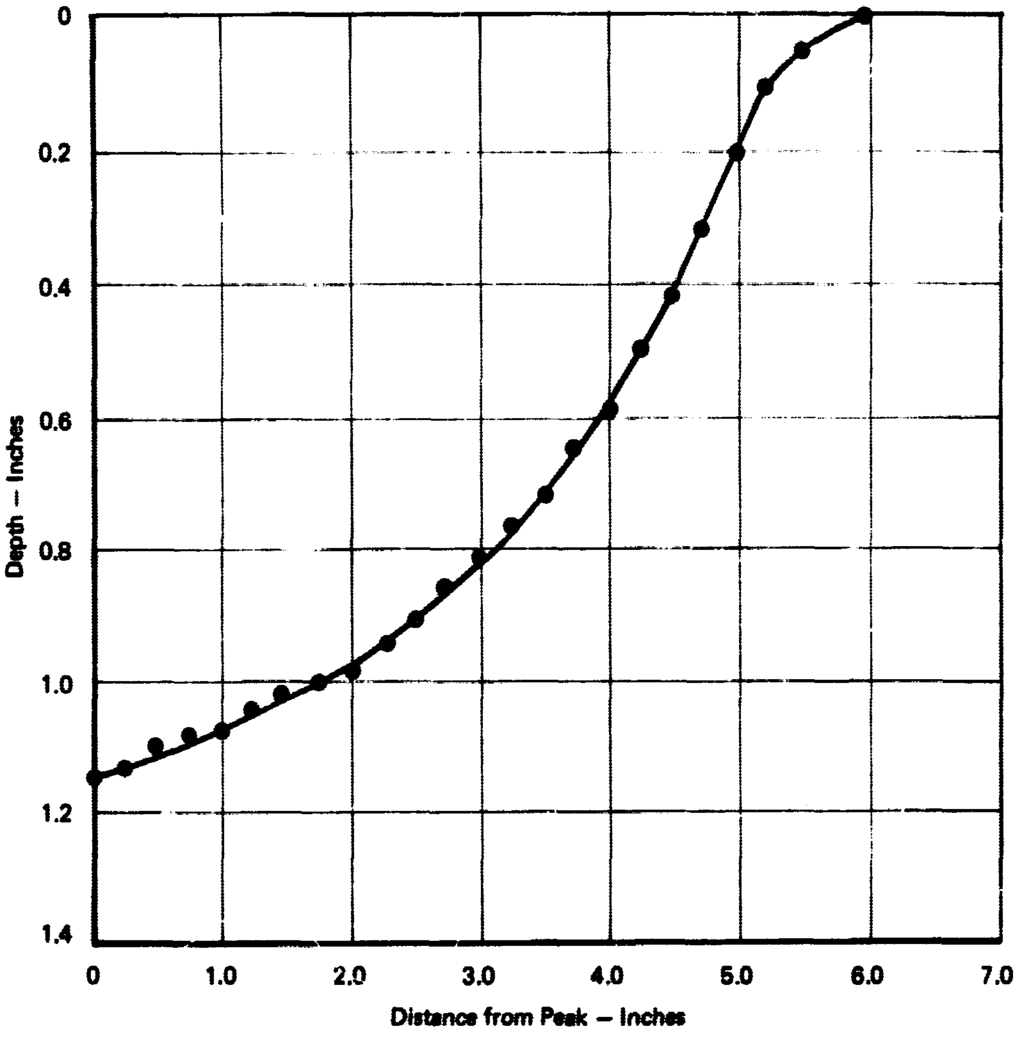

FIGURE 7 PROFILE OF EXPLOSIVELY FORMED SHEET TAKEN TRANSVERSE TO ROLLING DIRECTION ON THE CONCAVE SURFACE

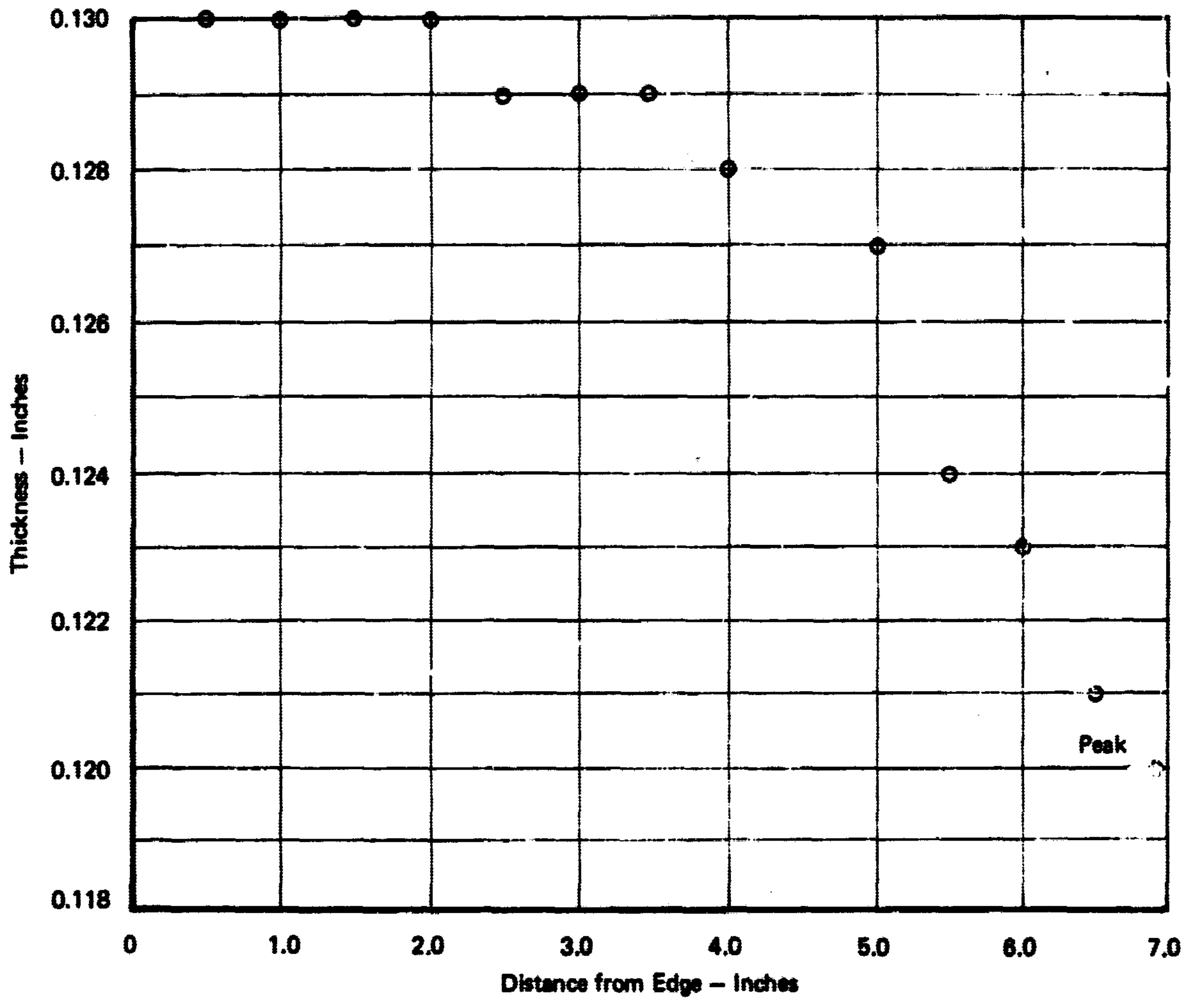

FIGURE 8 THICKNESS OF MAGNETOMOTIVELY FORMED SHEET NO. 12 TAKEN PARALLEL TO ROLLING DIRECTION

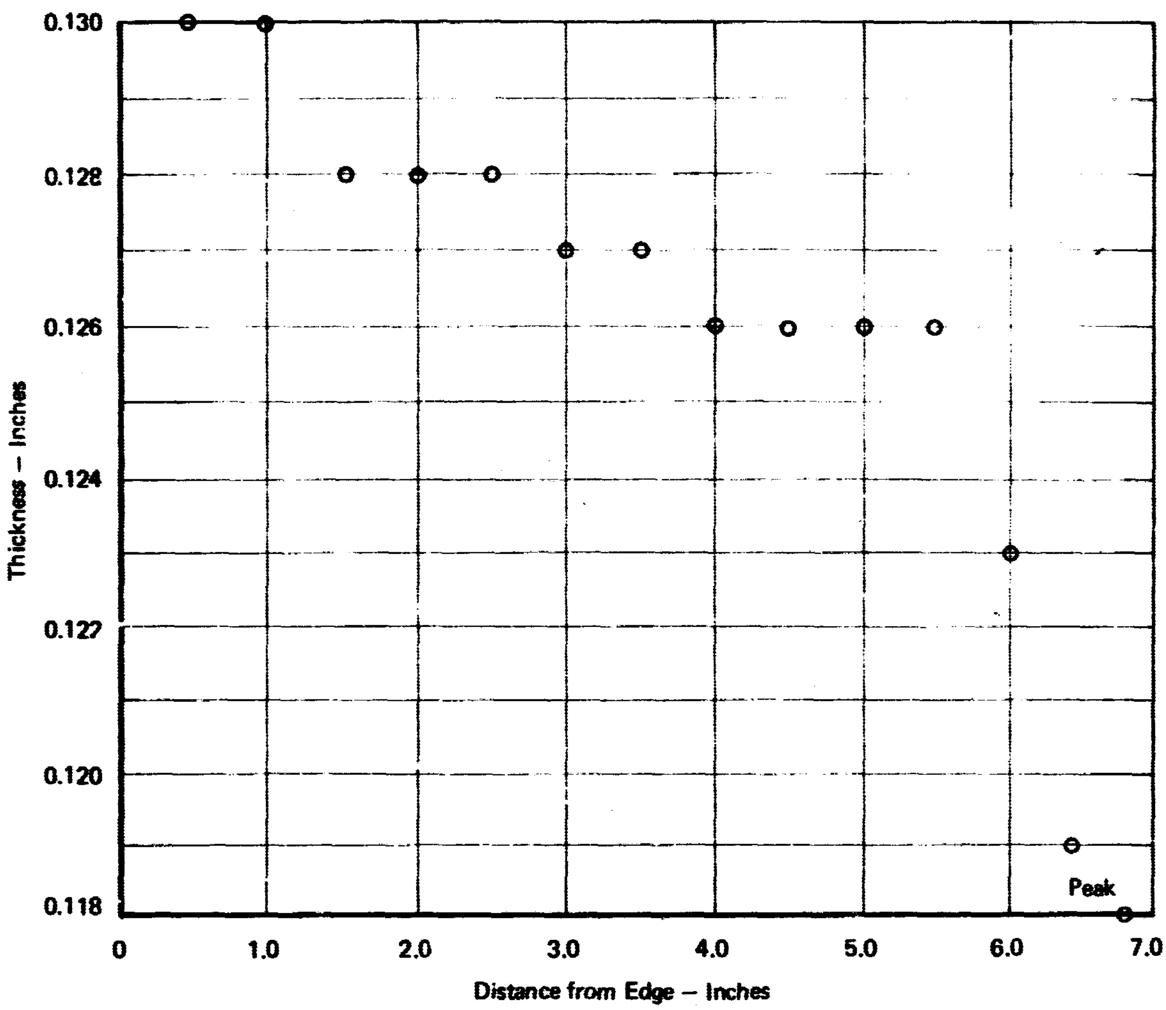

FIGURE 9 THICKNESS OF MAGNETOMOTIVELY FORMED SHEET NO. 12 TAKEN TRANSVERSE TO ROLLING DIRECTION

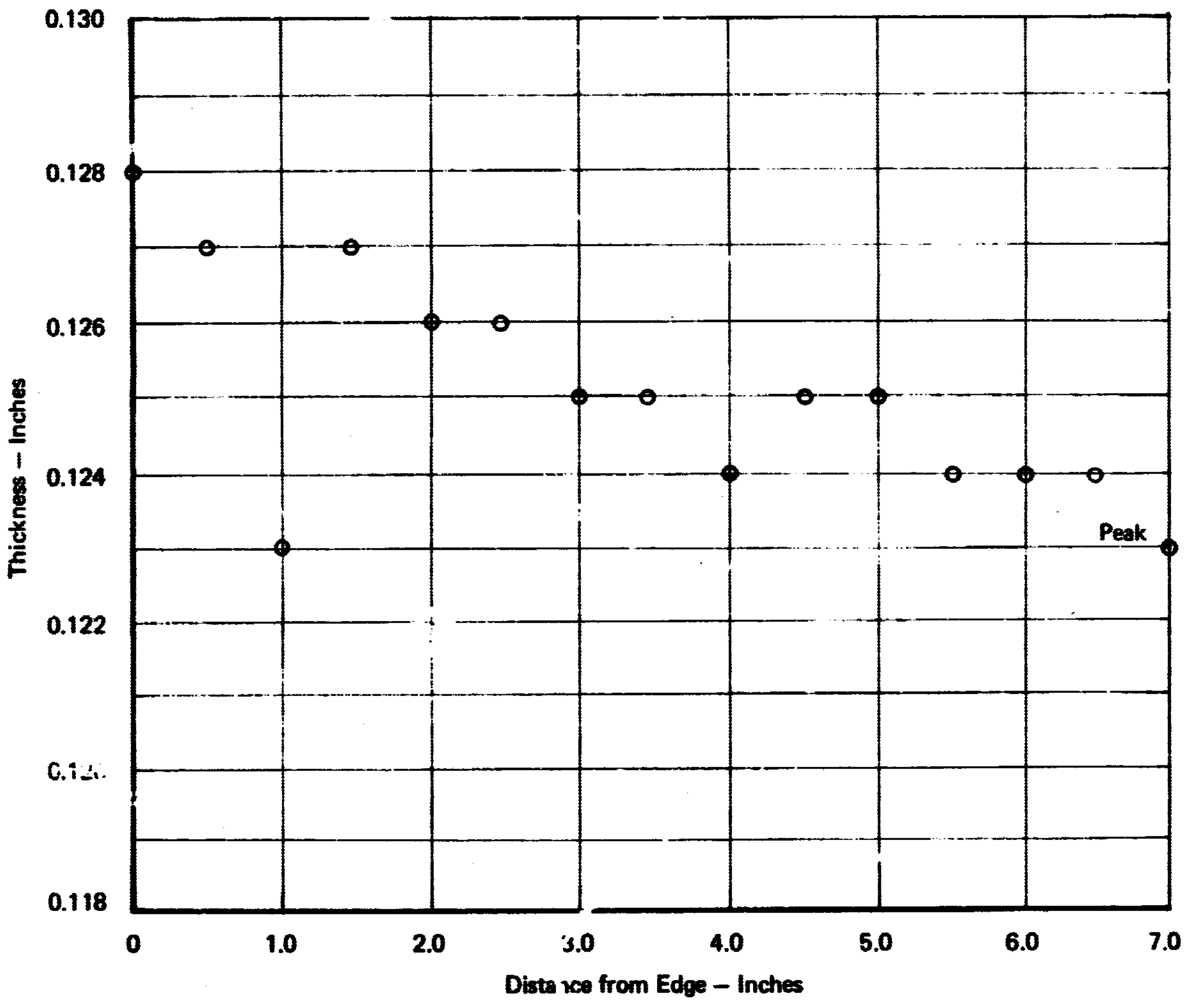

FIGURE 10 THICKNESS OF EXPLOSIVELY FORMED SHEET NO. 30 TAKEN PARALLEL TO ROLLING DIRECTION

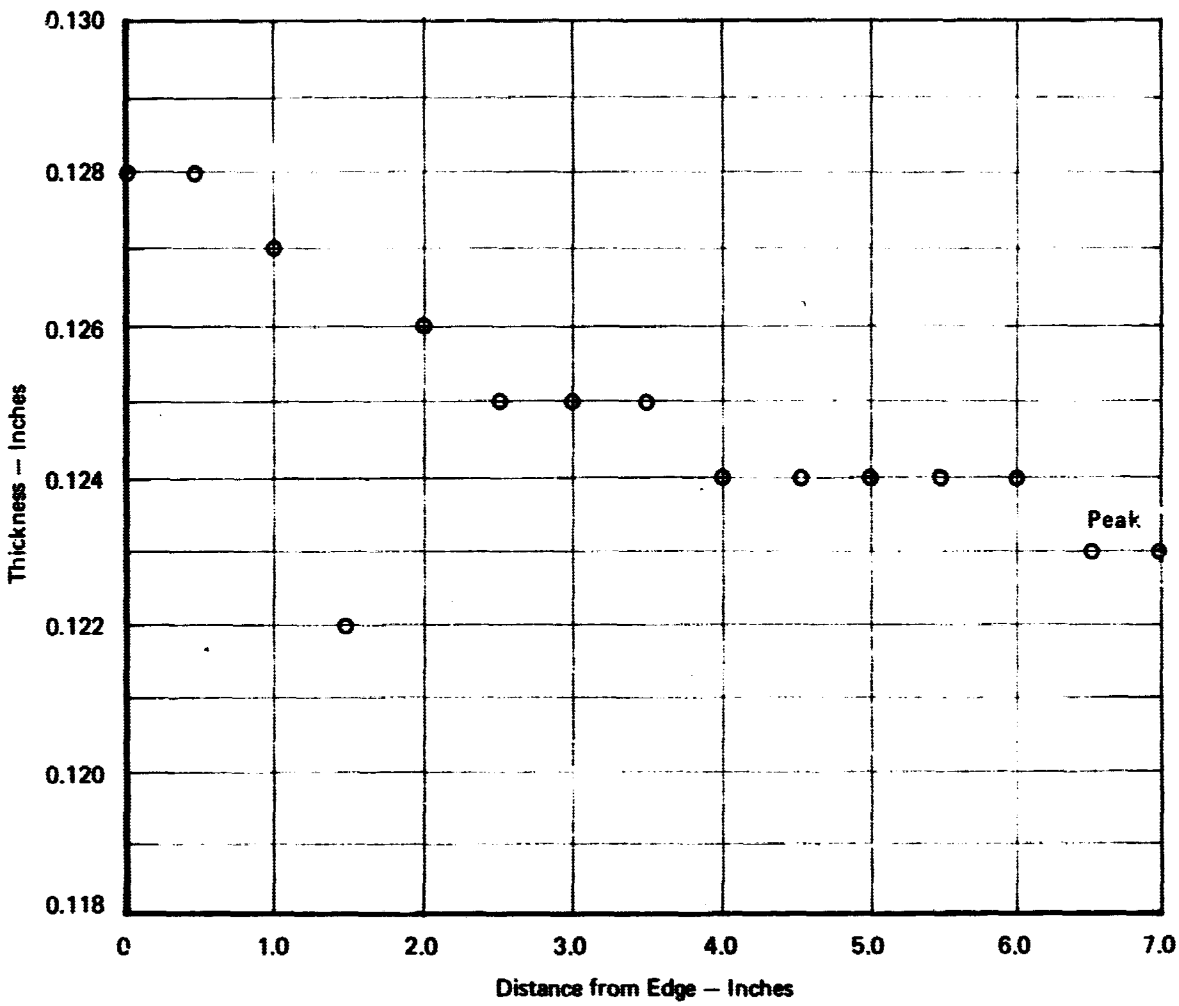

FIGURE 11 THICKNESS OF EXPLOSIVELY FORMED SHEET NO. 30 TAKEN TRANSVERSE TO ROLLING DIRECTION

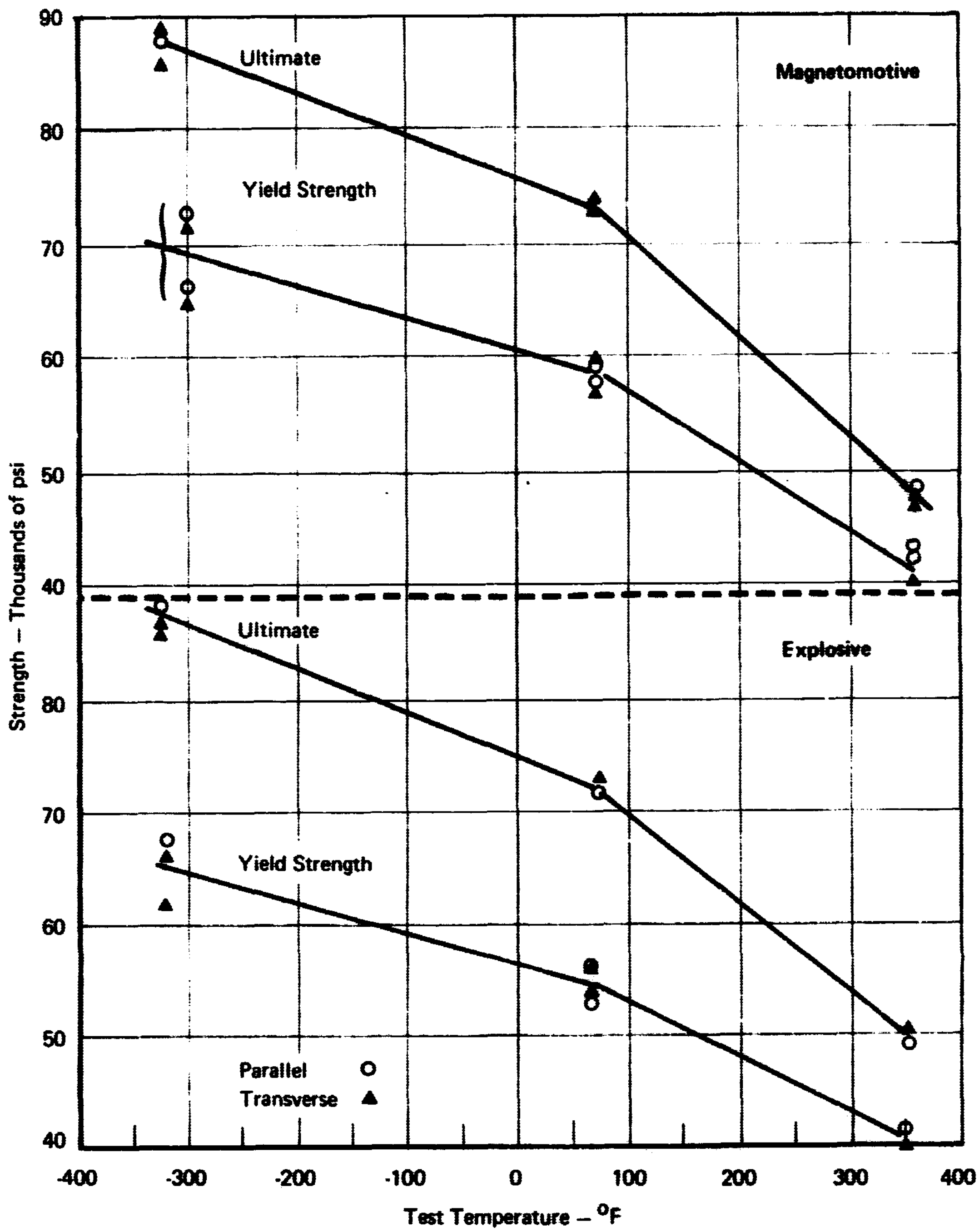

FIGURE 12 STRENGTHS OF MAGNETOMOTIVELY AND EXPLOSIVELY FORMED SHEETS AS A FUNCTION OF TEST TEMPERATURE

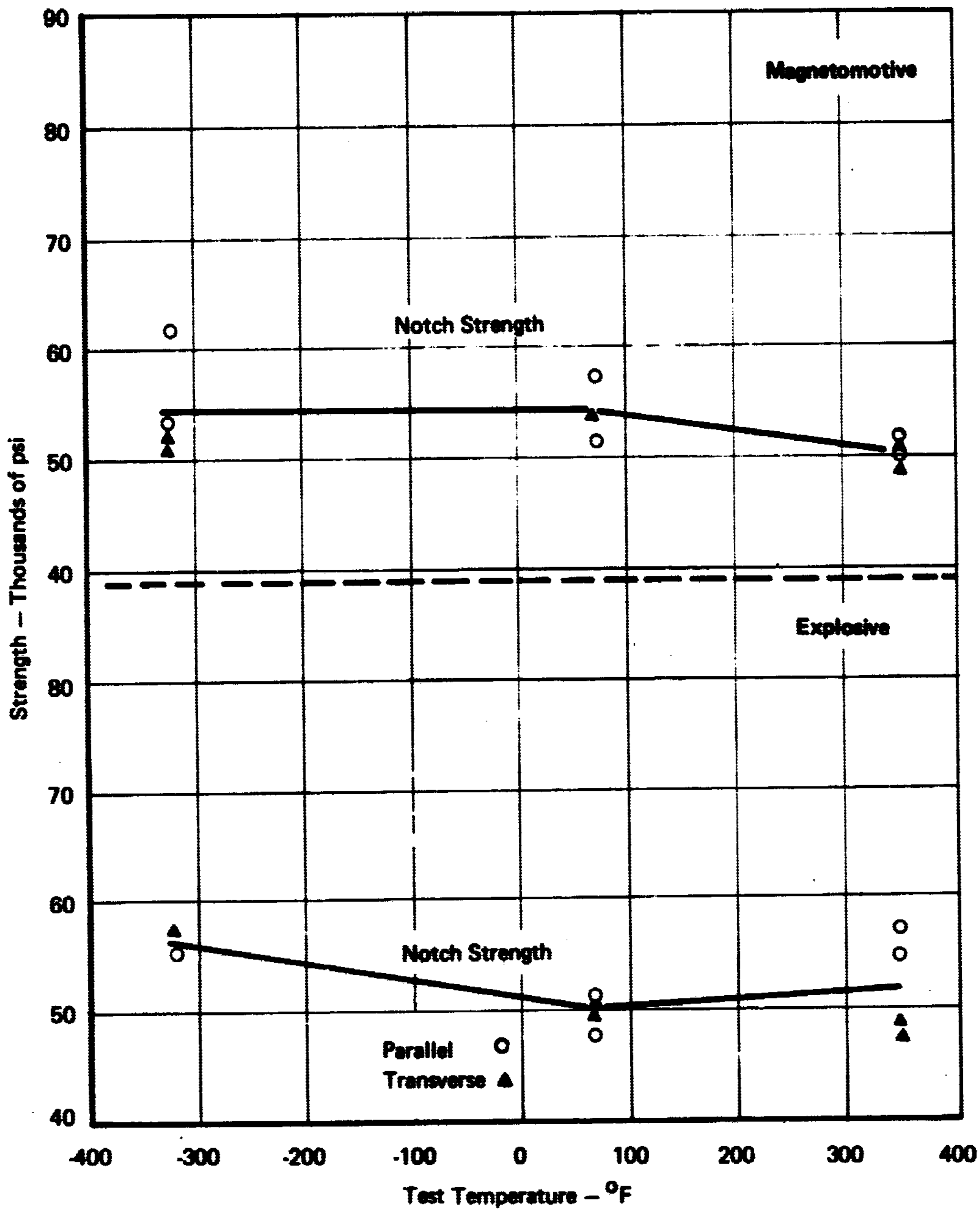

FIGURE 13 NOTCH STRENGTHS OF MAGNETOMOTIVELY AND EXPLOSIVELY FORMED SHEETS AS A FUNCTION OF TEST TEMPERATURE

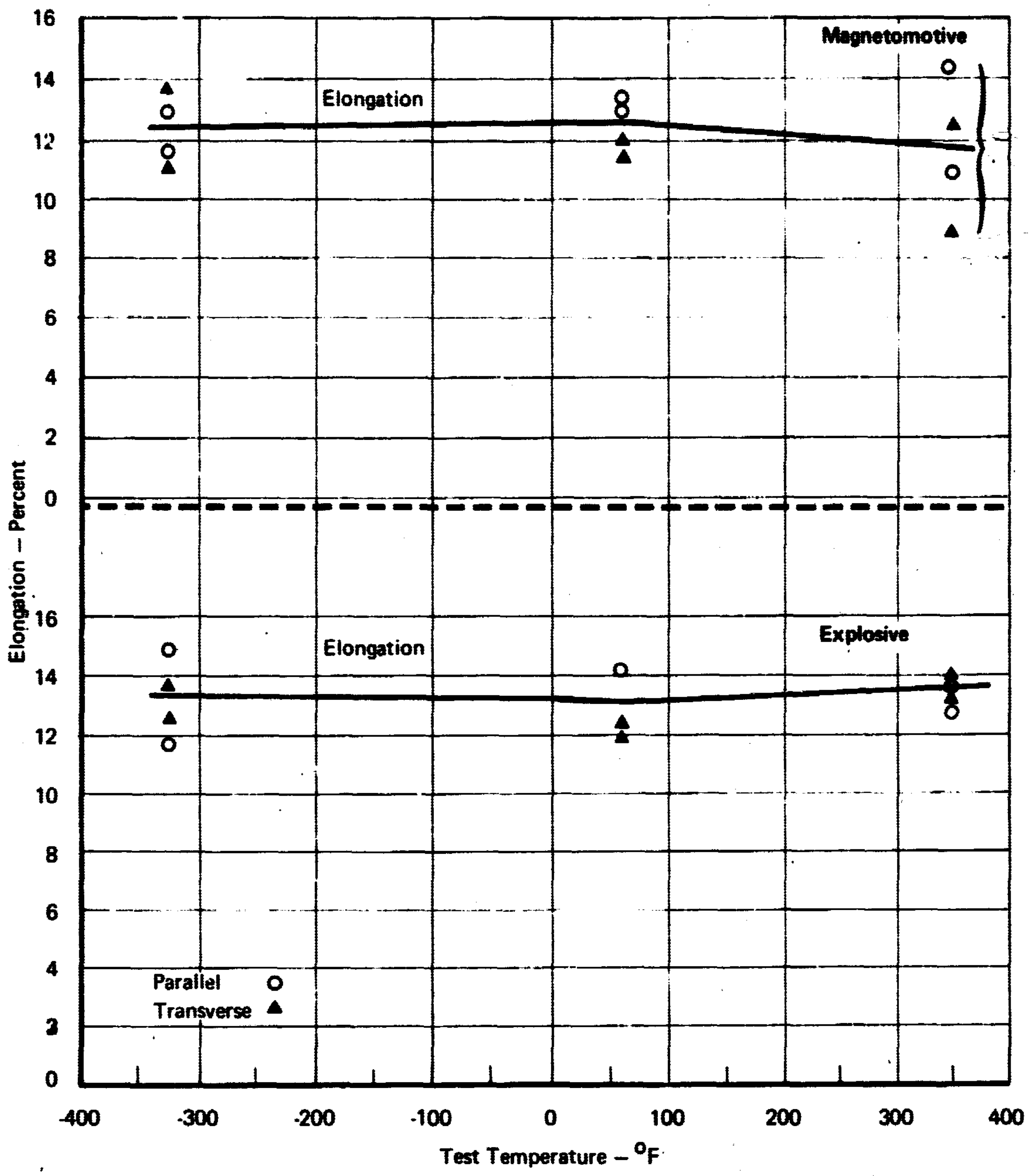

FIGURE 14 ELONGATIONS OF MAGNETOMOTIVELY AND EXPLOSIVELY FORMED SHEETS AS A FUNCTION OF TEST TEMPERATURE

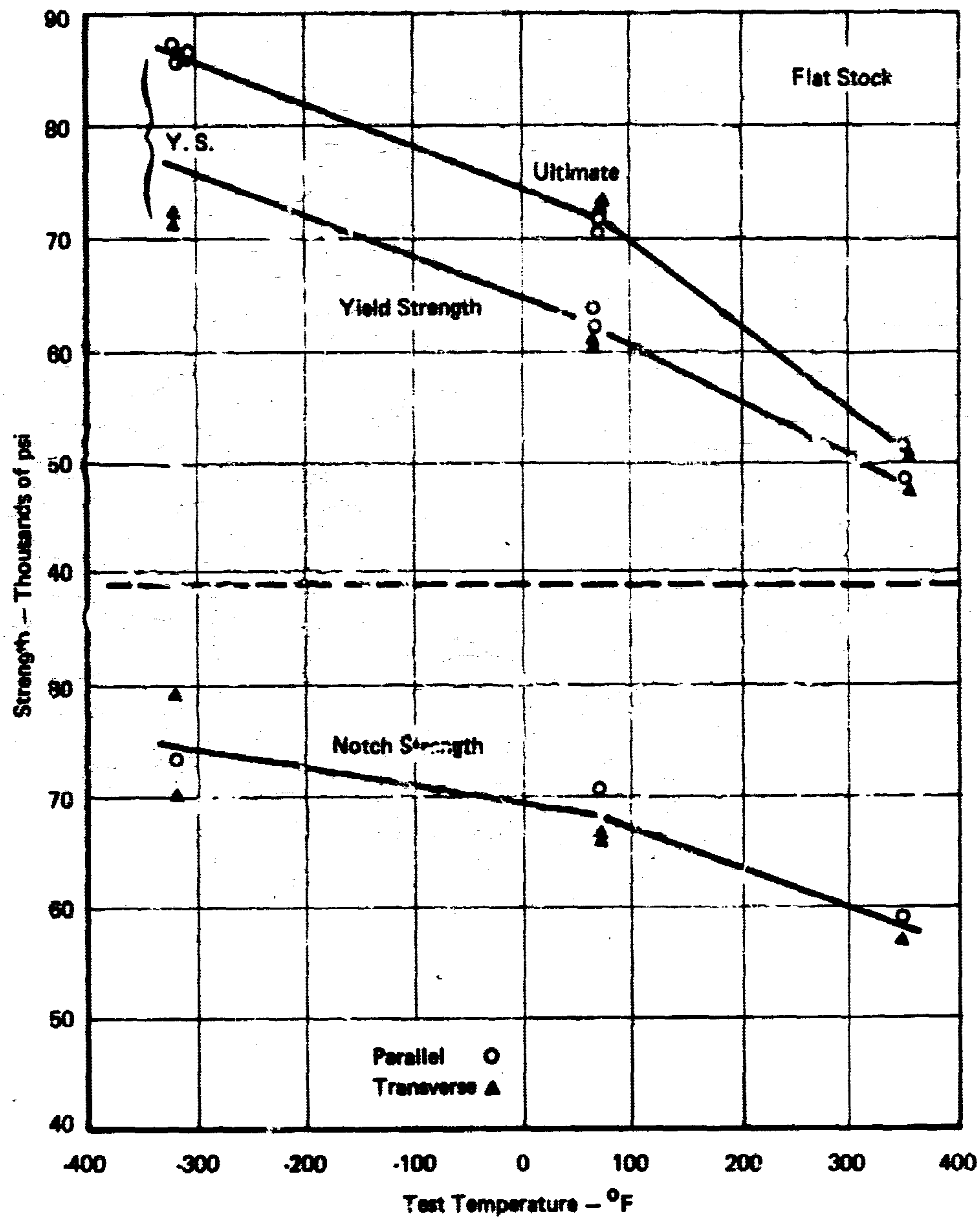

FIGURE 15 STRENGTHS AND NOTCH STRENGTHS OF THE FLAT STOCK AS A FUNCTION OF TEST TEMPERATURE

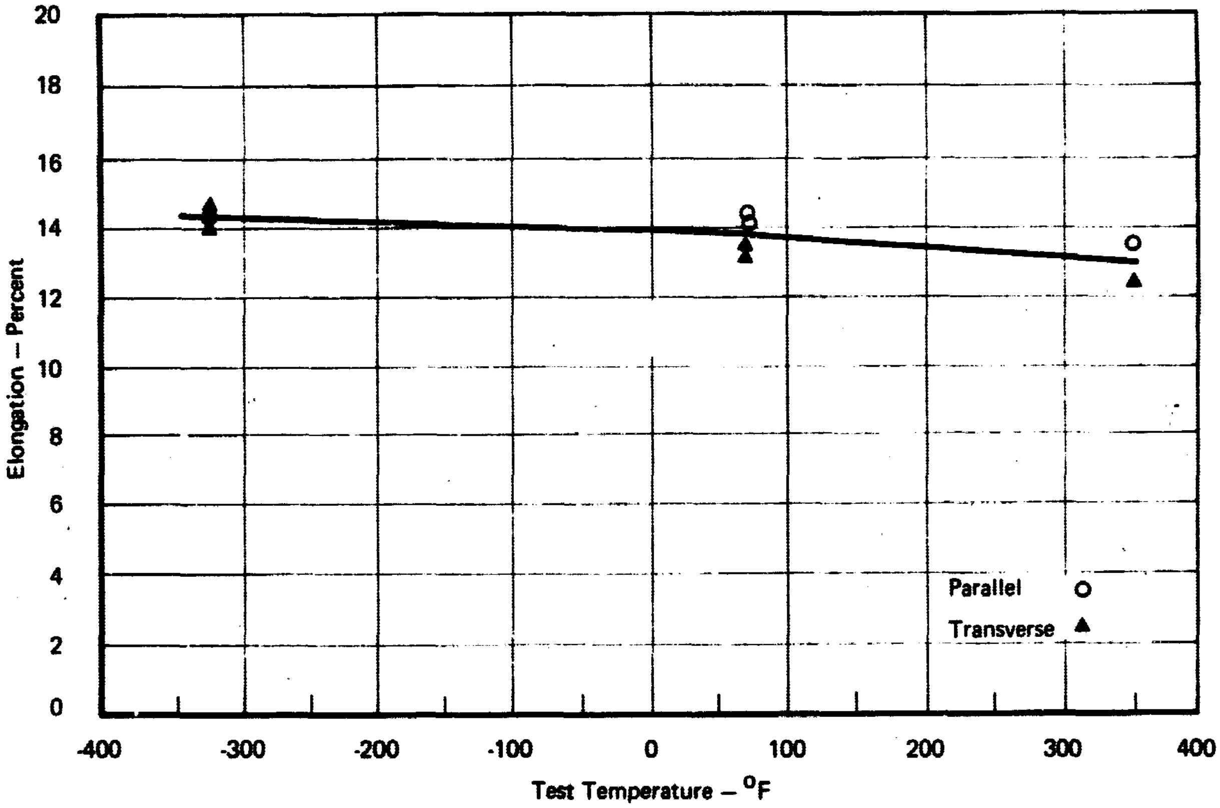

FIGURE 16 ELONGATIONS OF THE FLAT STOCK AS A FUNCTION OF TEST TEMPERATURE

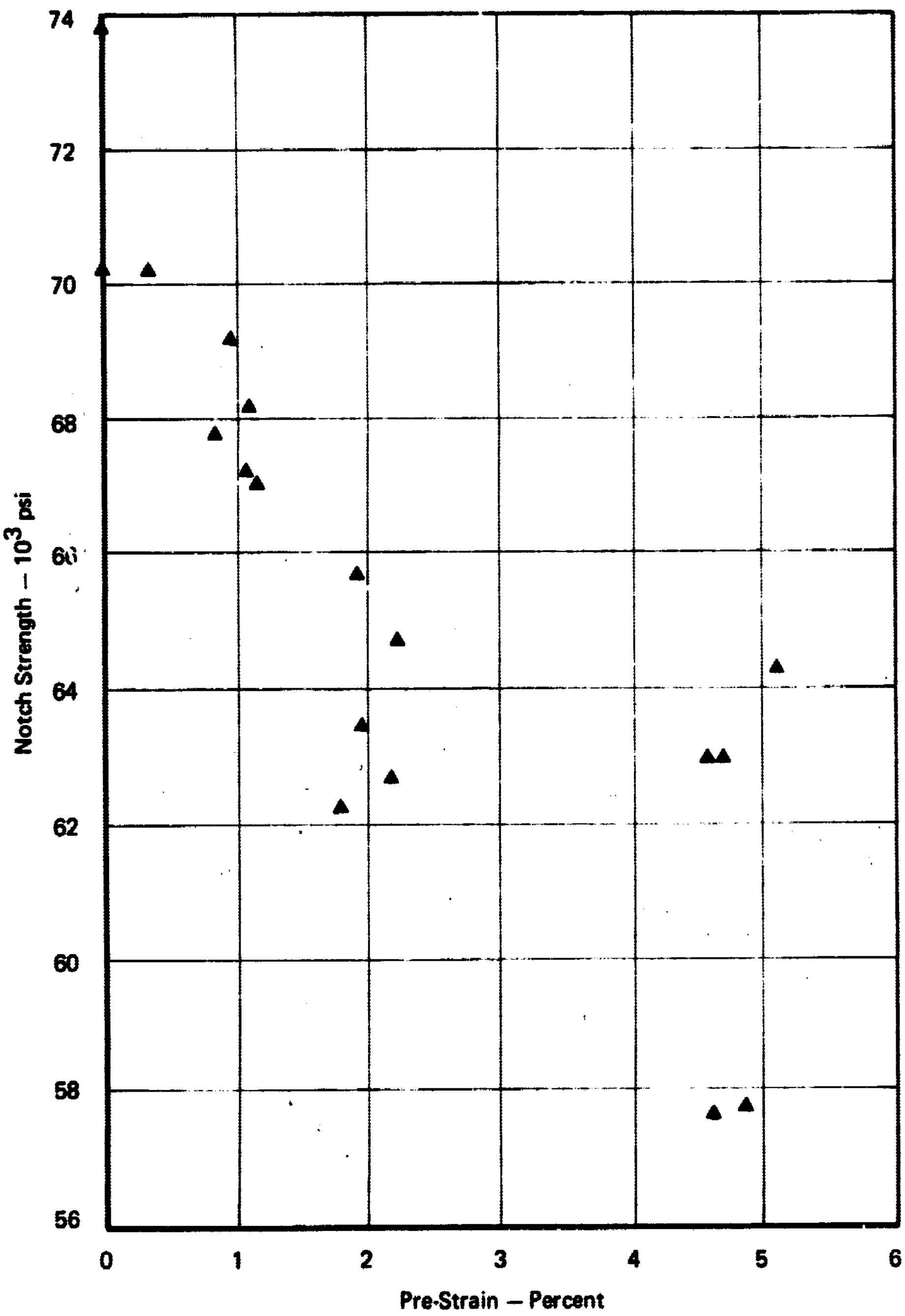

FIGURE 17 EFFECT OF PRE–STRAIN ON NOTCH STRENGTH

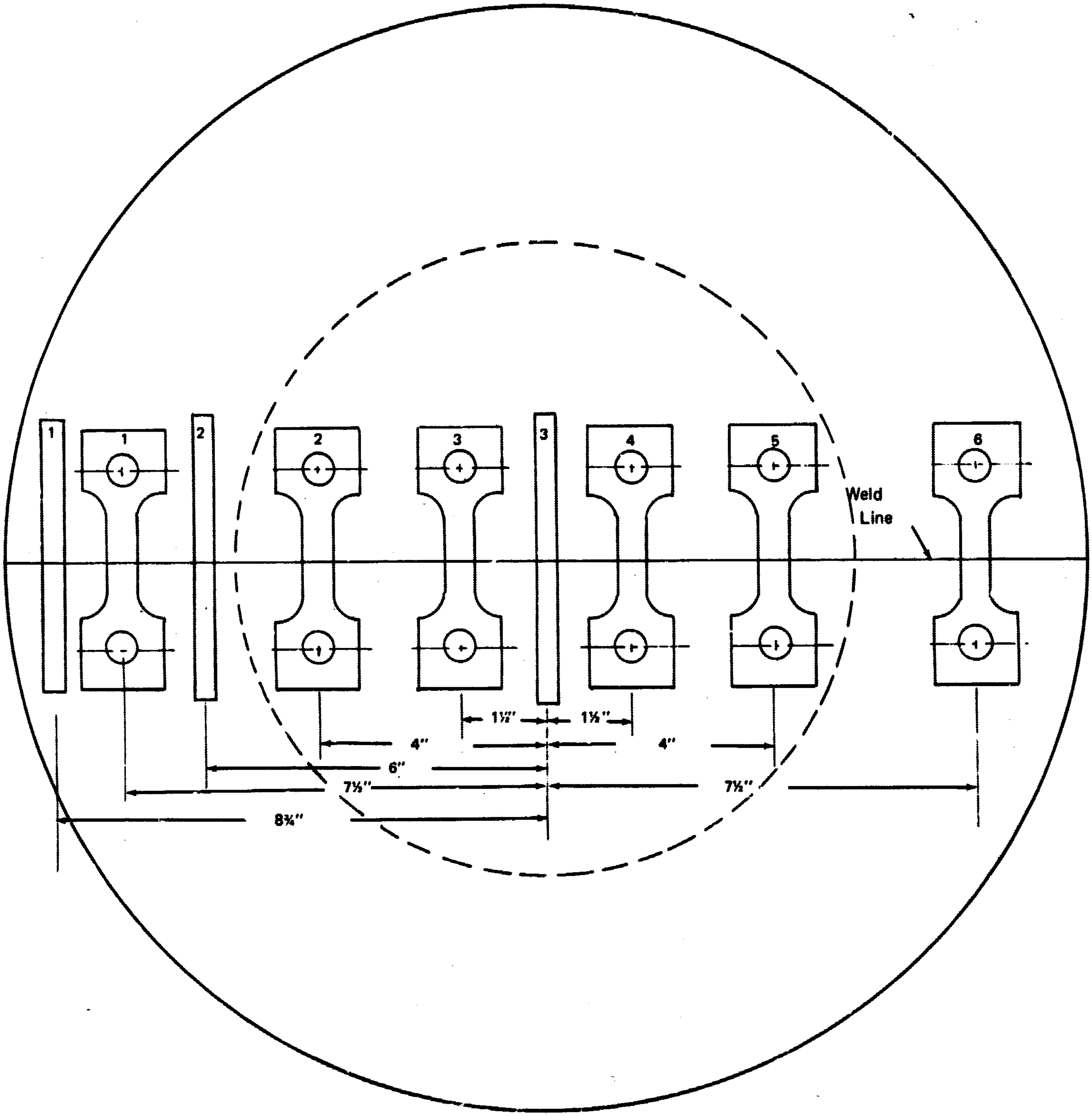

FIGURE 18 LOCATION OF SPECIMENS ON THE BULGED SHEET 5W

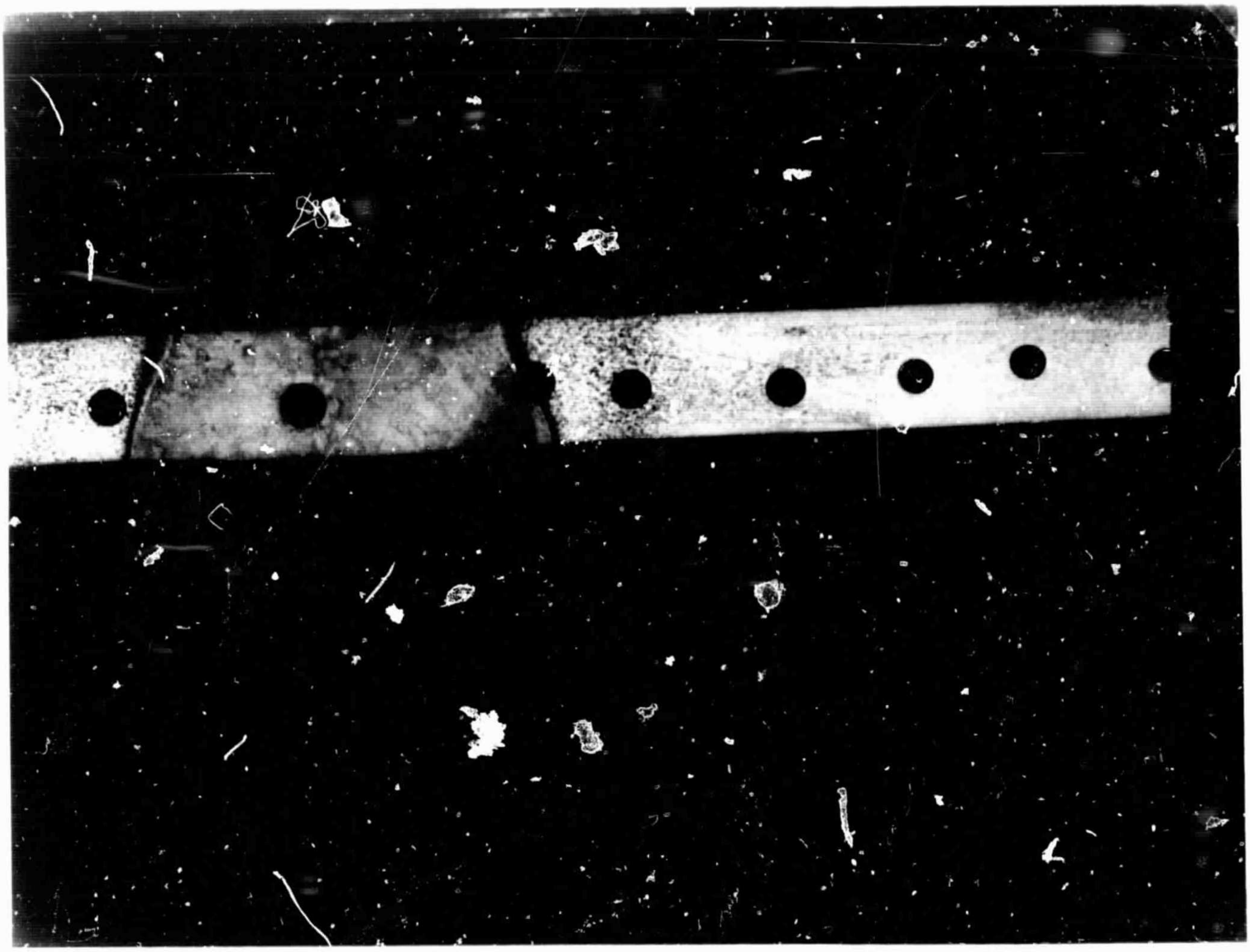

FIGURE 19 HARDNESS INDENTATIONS ON THE CROSS-SECTION OF WELDED PLATE 5W, SPECIMEN 1 (UNDEFORMED REGION) 3.5X

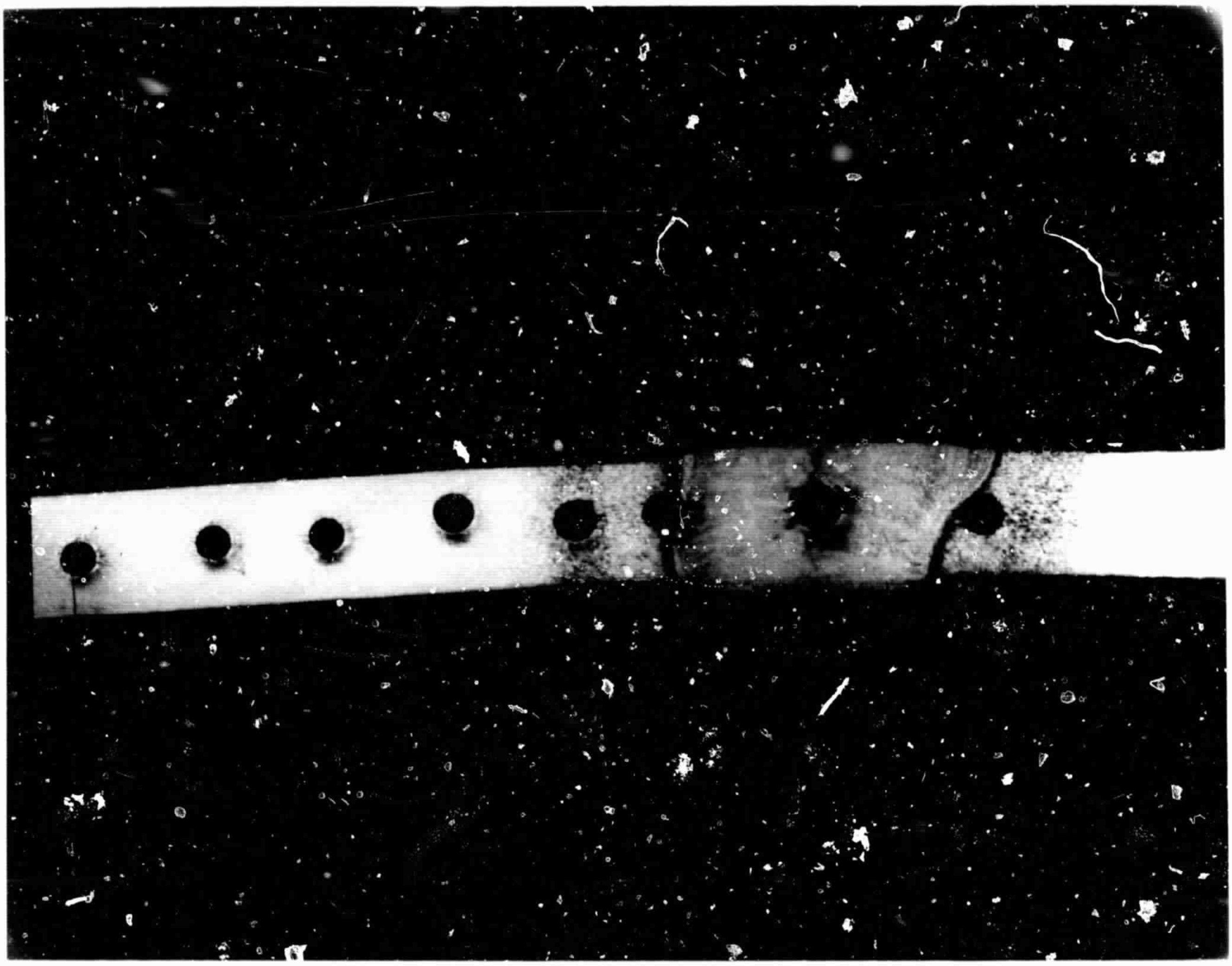

FIGURE 20 HARDNESS INDENTATIONS ON THE CROSS-SECTION OF WELDED PLATE 5W, SPECIMEN 3 (DEFORMED REGION) 3.5X

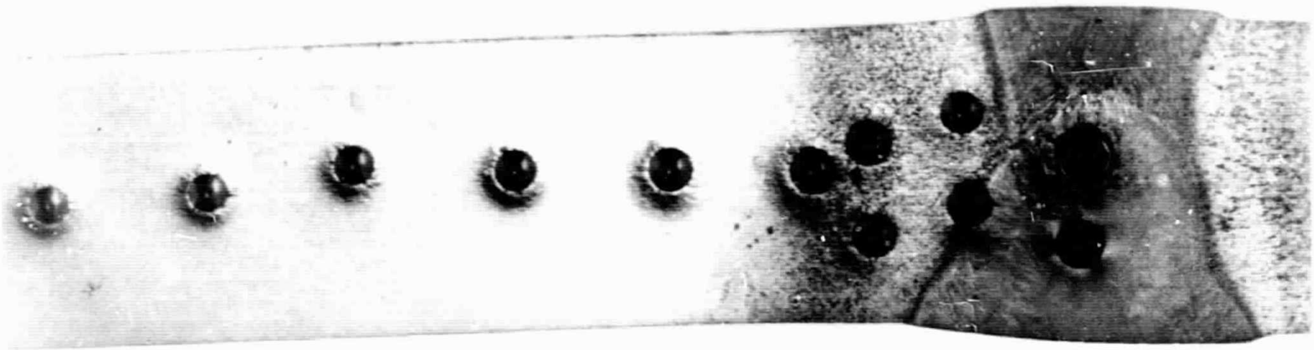

FIGURE 21 HARDNESS INDENTATIONS ON THE CROSS-SECTION OF WELDED PLATE C, 5X

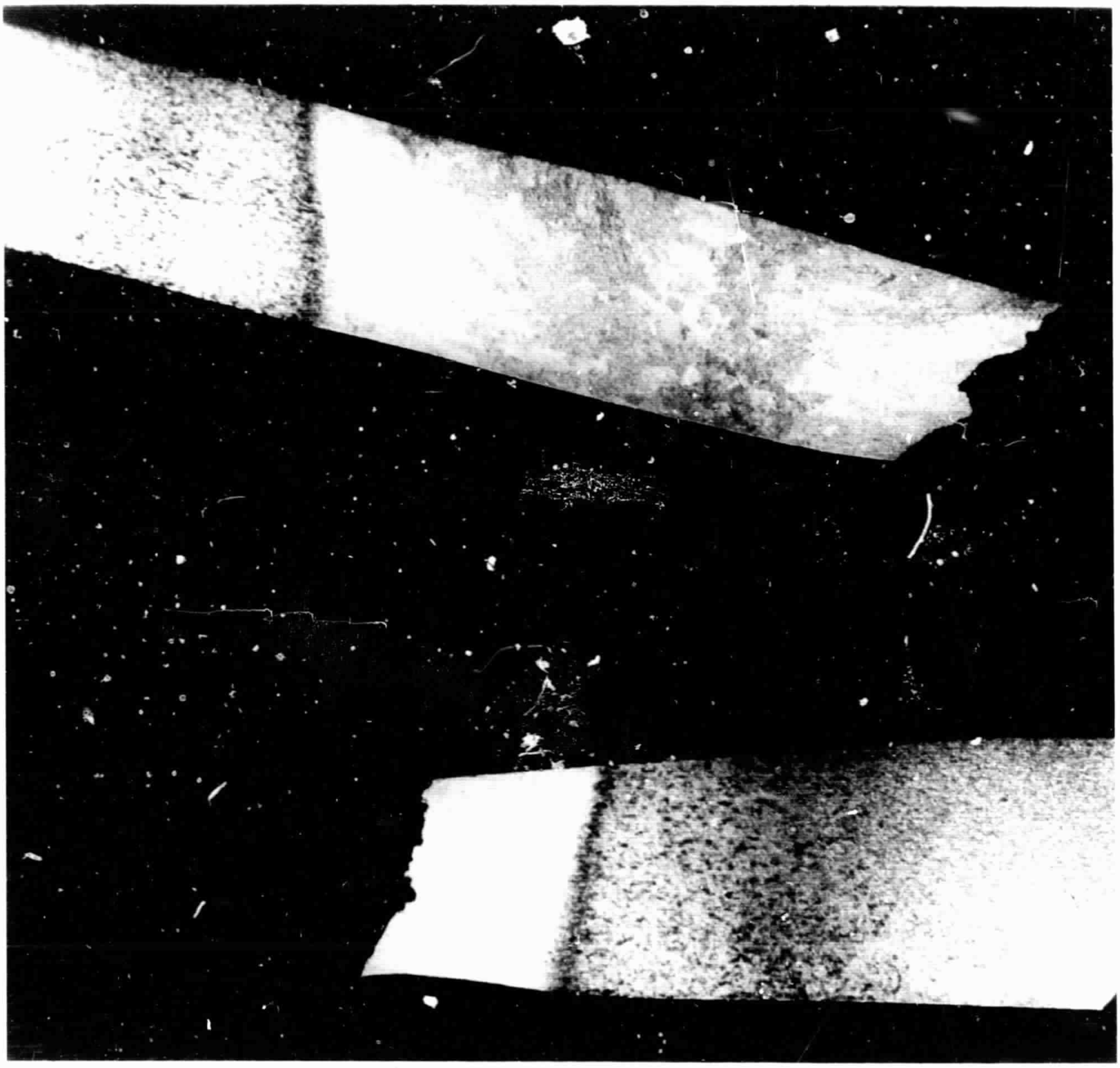

FIGURE 22 FRACTURED TENSILE SPECIMEN FROM PLATE 5W
CROSS-SECTIONAL VIEW

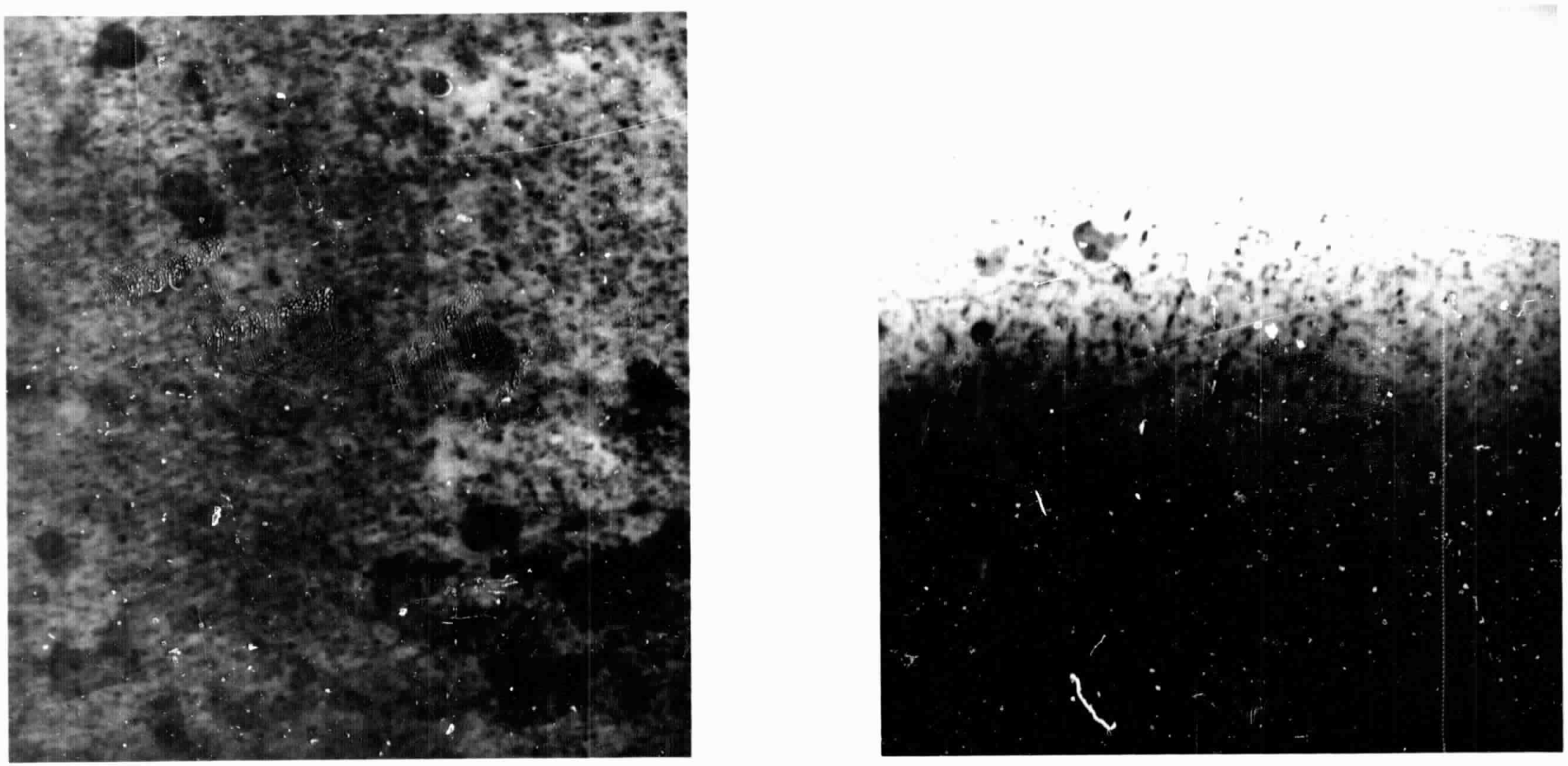

FIGURE 23 TRANSMISSION ELECTRON MICROGRAPH OF DEFORMED (A) AND UNDEFORMED (B) AREAS FROM SHEET 11. MAGNIFICATION 80,000X